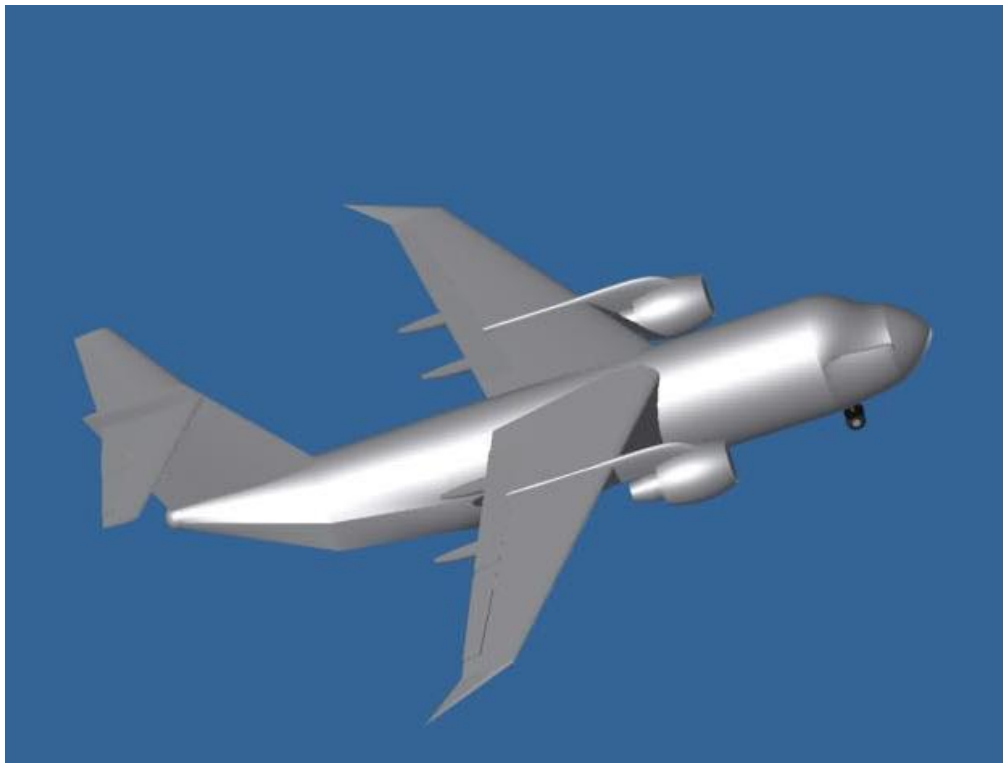


# A-TEAM AERONAUTICS

PRESENTS

## “MR. T”



Inter-Theater Tactical Transport with Austere STOL  
Capability  
2006-2007 AIAA Undergraduate Design Competition  
Virginia Polytechnic Institute and State University  
Aerospace Engineering  
April 30, 2007

## **EXECUTIVE SUMMARY**

The A Team presents the Mr. T as a solution to the 2006-2007 AIAA Team Undergraduate design Competition Request for Proposal for an Inter-Theatre Tactical Transport with Austere STOL Capability.

The purpose of this aircraft is to meet the requirements for a transport with Short Take-off Landing field capability to deliver a Future Deployable Armored Vehicle and support equipment to landing areas that were not dedicated air fields. It would need to be deployed from the Continental United States and integrate into the current international space system, meaning cruise at commercial speeds and altitudes.

Mr. T is a twin-engine aircraft that utilized high-mounted wings and an externally blown flap design, allowing the aircraft to fulfill the Short Takeoff Landing requirement. We have chosen the Pratt and Whitney 2043 high Bypass ratio turbofan mounted under the wings to provide airflow to the externally blow flaps. The fuselage and wings are composed of many materials, ranging from aluminum to titanium to carbon fiber epoxy composites. The different materials allow for a reduction in weight, ultimately allowing the aircraft to meet the 250 feet take off requirement set forth by the RFP. The fuselage shape is that of a traditional wedge shape with a T-tail, which allows for more predictable performance characteristics and improved pitch control. The tail also has double hinged control surfaces for increased control at lower speeds. The main landing gear is a quad bogey on each side of the aircraft with a tandem wheeled gear on the nose, constructed of titanium alloy. This material is strong and corrosive resistant, keeping the structural integrity to handle the loads of landing.

The Mr. T goes beyond the capabilities of any military transport of the United States Armed Forces fleet. With the ability to take off and land in under 2500 ft, cruise at the altitude and speed of commercial aircraft, and be used for both vehicle transportation and support materials, this aircraft will be able effectively fulfill all the requirement of the RFP, allowing the United States Armed Forces to have an aircraft that will transport the Future Deployable Vehicle to undesignated runways all over the world.

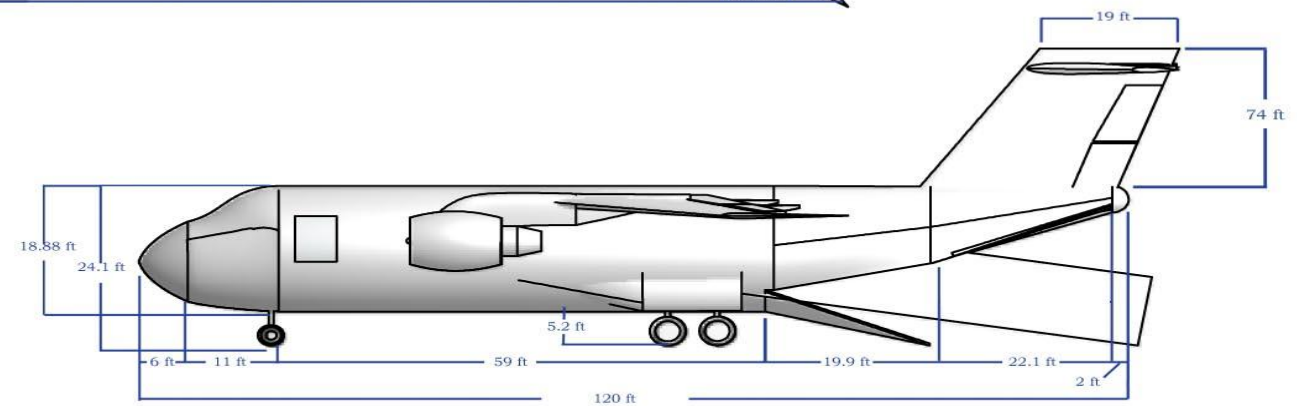
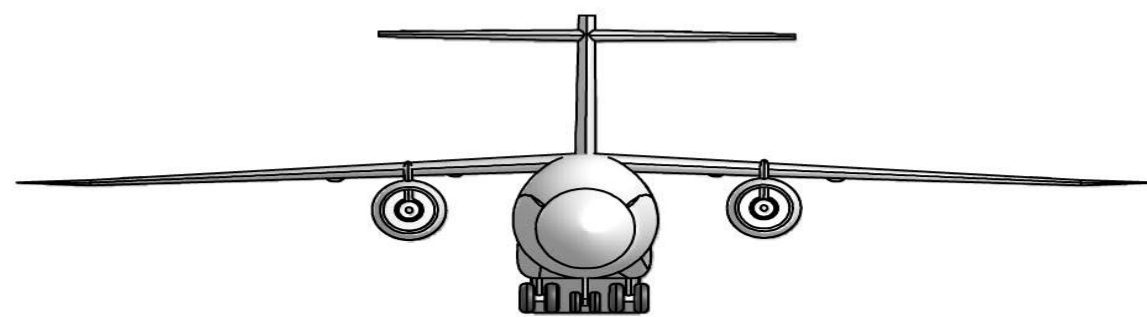
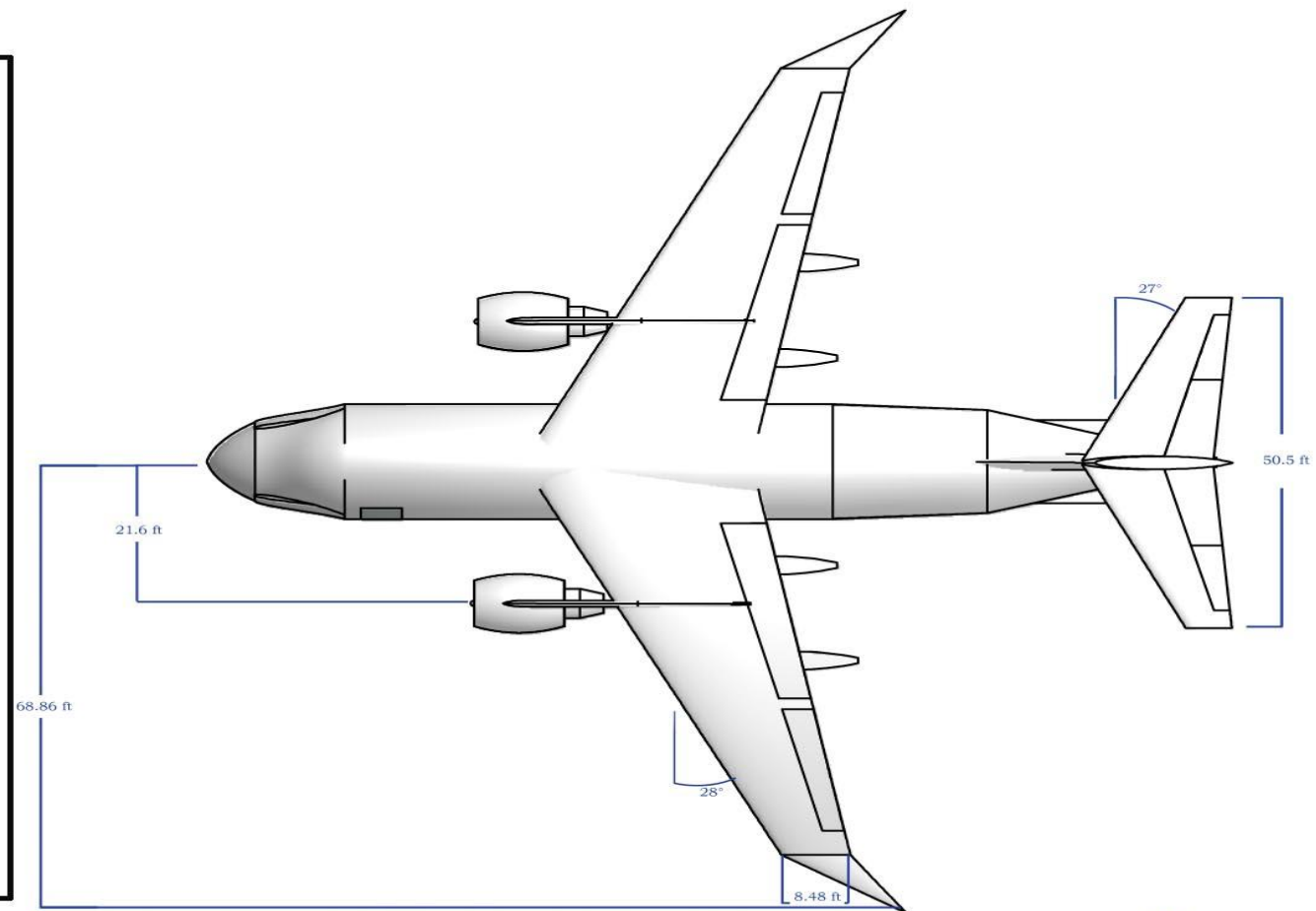
Surface	Area-ft <sup>2</sup>	Span	Root chord	Tip chord	AR	TR
WING	2576	137.72	28.25	8.48	7.0	0.3
HORIZ. TAIL						
VERT. TAIL						

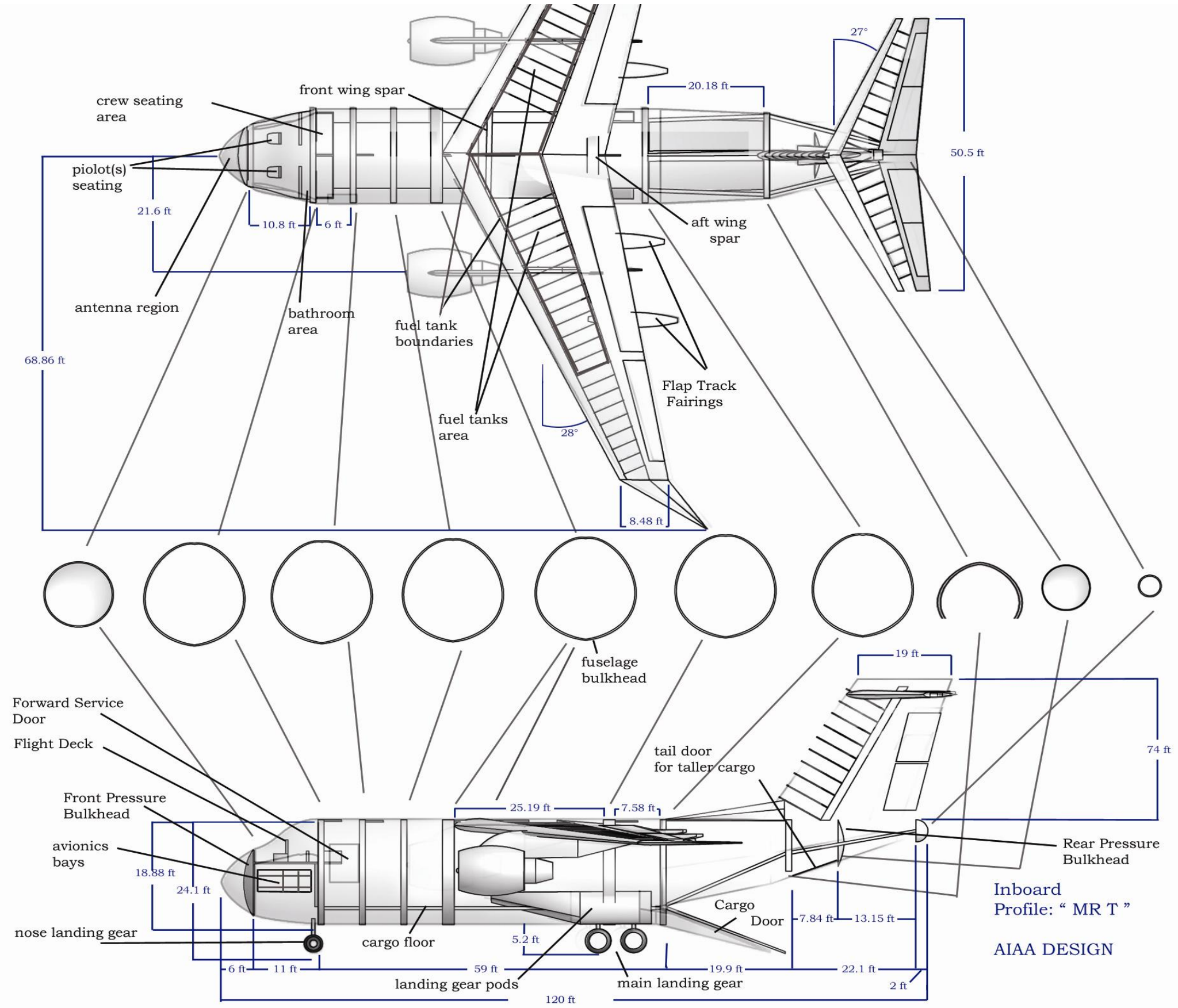
  

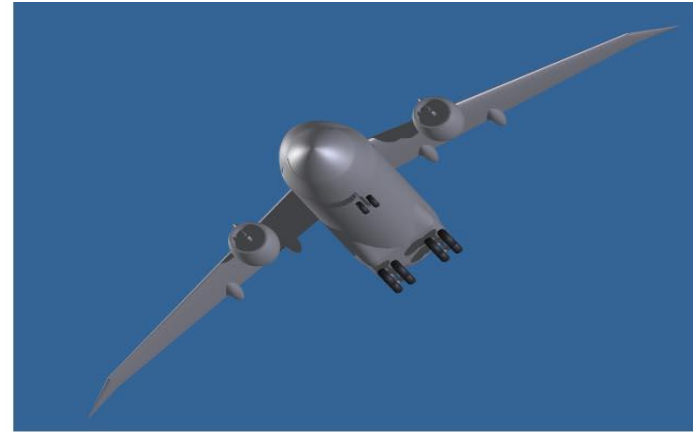
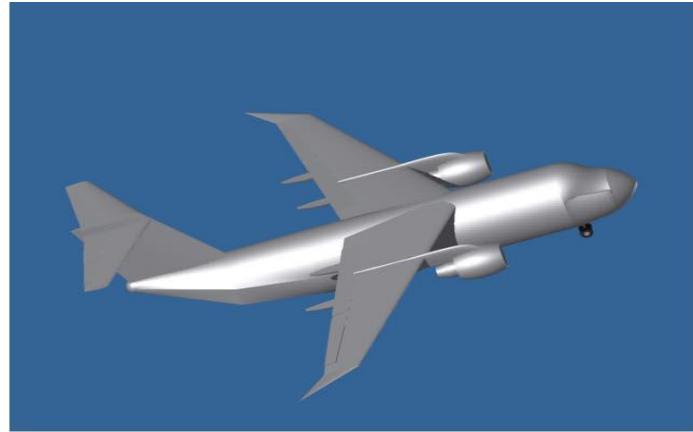
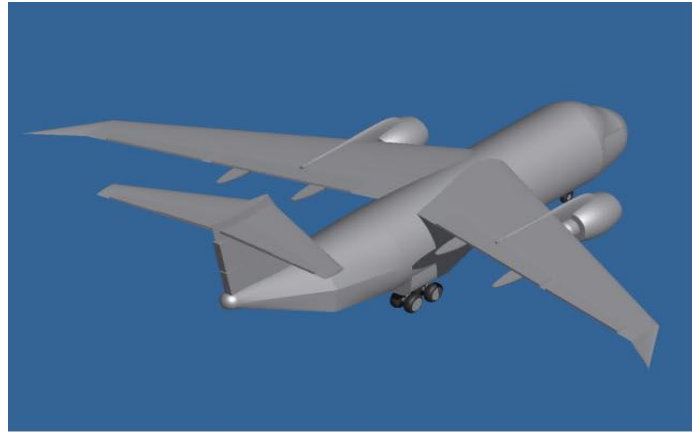
Surf. Controls	Area-ft <sup>2</sup>
AILERON	
SPOILER	
T.E. FLAPS	
L.E. FLAPS	
HORIZ. TAIL RUDDER	

Weights	Empty-lbs	Useful Load-lbs	TOGW-lbs	Fuel Load-lbs
	101,111	60,555	226,666	65,000







# TABLE OF CONTENTS

Executive Summary .....	i
Table of Contents .....	vi
List of Figures .....	x
List of Tables .....	xii
List of Abbreviations .....	xiii
List of Symbols .....	xiv
The A-Team .....	xvi
1. Preliminary Design .....	1
1.1 Introduction.....	1
1.1.1 Design Requirements .....	1
1.1.2 Required Missions .....	2
1.2 Configurations.....	3
1.2.1 Considered Configurations .....	3
1.3 Comparable Aircraft .....	6
1.4 Design Strategy.....	6
1.5 Final Selection .....	7
2. Configuration .....	9
3. Weight and Balance .....	11

3.1 Constraint Diagram.....	11
3.2 Sizing .....	12
3.3 Weight Breakdown of Mr. T.....	15
3.4 Fuel Weight Analysis.....	17
4. Aerodynamics .....	19
4.1 General Wing Configuration Factors.....	19
4.2 T-tail Configuration .....	19
4.3 Wing Planform Selection.....	20
4.4 Twist Distribution .....	22
4.5 Airfoil Selection.....	22
4.6 Friction and Form Drag .....	25
4.7 Drag Polars at Cruise .....	25
4.8 Cruise Drag .....	27
4.9 Coefficient of Lift at Take-off .....	27
4.10 High Lift Systems .....	28
4.11 Leading Edge Lifting Devices .....	31
4.12 Drag Polars for Take-off and Landing Conditions .....	31
4.13 Effect of Externally Blown Flaps on Pitching Moment.....	33
5. Propulsion .....	34

5.1 Introduction.....	34
5.2 Engine Selection .....	34
5.3 Engine Performance.....	38
5.4 Engine Out .....	40
6. Stability and Control.....	42
6.1 Stability and Control Derivatives.....	42
6.2 Center of Gravity Variation .....	44
6.3 Deep Stall.....	45
7. Performance .....	47
7.1 Requirements .....	47
7.2 Overview.....	47
7.3 Takeoff.....	50
7.4 Landing .....	52
8. Structure and Materials.....	55
8.1 Structural Configurations and Materials.....	55
8.2 Load Limit .....	55
8.3 Materials .....	56
8.4 Internal Structure .....	59
8.4.1 Fuselage .....	60

8.4.2 Wings ..... 61

8.4.3 Empennage..... 61

8.4.4 Nacelles ..... 62

8.4.5 Landing Gear ..... 62

9. Systems ..... 64

9.1 Flight Control Systems ..... 64

9.2 Avionics ..... 64

9.3 Navigation..... 65

9.4 Communications ..... 65

9.5 Fuel tanks ..... 65

9.6 Refueling..... 66

9.7 Environment and Electric Systems ..... 67

9.8 Air Defense Systems and Safety..... 67

9.9 Noise Mitigation ..... 68

9.10 Lavatory ..... 69

10. Costs..... 70

11. Conclusion ..... 73

Works Cited ..... 76

# LIST OF FIGURES

Figure 1.1 – FDAV Combat Mission Profile.....	2
Figure 1.2 – Transoceanic Ferry Mission Profile.....	3
Figure 1.3 – High wing, conventional tail, 4 low-mounted engines.....	4
Figure 1.4 – High wing, T-Tail, 2 low-mounted engines.....	4
Figure 1.5 – High wing, T-Tail, 3 high-mounted engines.....	5
Figure 3.1 – Constraint Diagram.....	11
Figure 3.2 - T-tail WE vs. TOGW.....	14
Figure 3.3 - Conventional Tail WE vs. TOGW.....	14
Figure 3.4 - Optimal Design of W/S vs. T/W at $C_{L_{max}}$ .....	15
Figure 4.1 - Wing Planform Area, T-tail Aircraft.....	21
Figure 4.2 - Mr. T Wing Twist Distribution.....	22
Figure 4.3 – Cp Distribution at Cruise.....	24
Figure 4.4 - Drag polar for the Untrimmed Cruise Condition.....	26
Figure 4.5 - Drag polar for the Trimmed Cruise Condition.....	27
Figure 4.6 - Triple-slotted Flaps.....	29
Figure 4.7 - Externally Blown Flaps.....	29
Figure 4.8 - CL vs. angle of attack curve for externally blown flaps.....	30
Figure 4.9 – Drag Polar for Take-off.....	32
Figure 4.10 – Drag Polar at Landing.....	32
Figure 4.11 – Pitching Moment Coefficient Curve.....	33
Figure 5.1 – PW2043 Engine Performance.....	39
Figure 5.2 – PW2043 Engine Performance.....	39
Figure 5.3 – Climb Gradient for PW2043.....	41
Figure 6.1 – Trim for CLmax for Various Elevator Deflections .....	43
Figure 6.2 - Primary Mission Center of Gravity .....	44
Figure 6.3 - Secondary Mission Center of Gravity Location.....	45
Figure 6.4 – Deep Stall of Mr. T.....	46
Figure 7.1 - Breakdown of takeoff segment.....	50
Figure 7.2 - X, Y Distances and Velocities vs. Time.....	52
Figure 7.3 - Breakdown of landing segment.....	52

Figure 8.1 - Vn Diagram.....	55
Figure 8.2 – Materials Placement.....	58
Figure 8.3 - Internal Structure.....	59
Figure 8.4 – Bulkheads.....	60
Figure 8.5 – Landing Gear.....	63
Figure 9.1 – Fuel Tanks.....	66

## **LIST OF TABLES**

Table 1.1 - RFP Requirements.....	2
Table 1.2 – Comparable Aircraft Chart.....	6
Table 1.3 – Design Evaluation Matrix.....	7
Table 3.1 - System Weights.....	13
Table 3.2 – Weight Breakdown of Mr. T.....	16
Table 3.3 – Moments of Inertia of Mr. T.....	17
Table 3.4 – Mission Profile Table for T-Tail.....	18
Table 4.1 – Wing Geometry, T-tail Aircraft.....	21
Table 4.2 – Friction and Form Drag Calculations.....	25
Table 5.1 – Engine Comparison.....	35
Table 5.2 – PW 2043 Information.....	37
Table 5.3 – Engine Out Condition.....	40
Table 6.1 – Stability and Control Values for Mr.T at Flight Conditions.....	42
Table 7.1 – Performance Estimates for Combat Mission.....	48
Table 7.2 – Performance Estimates for Ferry Mission.....	49
Table 7.3 – Normal Takeoff Performance.....	51
Table 7.4 – Normal Landing Performance.....	54
Table 8.1 – Characteristics of Materials.....	58
Table 10.1 – Constants for Costs Analysis.....	70
Table 10.2 – RDT&E Cost Analysis for 150, 500, and 1500 aircraft.....	71
Table 10.3 – Flyaway Cost Analysis for 150, 500, and 1500 aircraft.....	71
Table 10.4 – RDT&E + Flyaway Costs for 150, 500, and 1500 aircraft.....	72
Table 11.1 – Compliance to Design Drivers.....	74

## **LIST OF ABBREVIATIONS**

AAA	Advanced Aircraft Analysis
AIAA	American Institute of Aeronautics and Astronautics
APU	Auxiliary power Unit
BFL	Balanced Field Length
CBR	California Bearing Ratio
EGPWS	Enhanced Ground Proximity Warning System
EMI	electromagnetic interference
ETOPS	Extended-range Twin-engine Operations
FAA	Federal Aviation Administration
FAR	Federal Aviation Regulations
FADEC	Full-Authority Digital Electronic Control
FBL	Fly-by-Light
FDAV	Future Deployable Armored Vehicle
HUD	Head up Display
IFF	Identification Friend or Foe
MFRD	Multi-Function Radar Display
NASA	National Aeronautics and Space Administration
OBIGGS	On-Board Inert Gas Generation System
RFP	Request for Proposal
RTC	Reduce Temperature Configuration
STOL	Short take-off and Landing
TOGW	Take-off Gross Weight

## LIST OF SYMBOLS

$C_L$	Lift coefficient
$C_{L_{max}}$	Maximum lift coefficient
$C_D$	Drag coefficient
$C_{do}$	Parasite Drag
$C_{df}$	Friction Drag
$C_m$	Moment coefficient
$C_n$	Yaw moment due to slide slip
$C_l$	Roll moment due to slide slip
$C_y$	Side force due to slide slip
$C_p$	Pressure coefficient
$C_\mu$	Thrust coefficient
$C_r$	Root chord
$C_t$	Tip chord
C.G	Center of Gravity
D	Drag
WE	Empty Weight
LE	Leading edge
TE	Trailing edge
MAC	Mean Aerodynamic Chord
t/c	Thickness ratio
SFC	Specific Fuel Consumption
S	Surface Area

$N_{TOEI}$	Engine out yaw moment
$\delta_r$	Aileron deflection
$D_{OEI}$	Engine out drag
W/S	Wing loading
T/S	Thrust to weight ratio
AR	Aspect ratio
b	Wing span
$\beta$	Side slip angle
L/D	Lift to drag ratio
q	Dynamic pressure
$\delta_e$	Elevator Deflection
$\delta_r$	Rudder Deflection
$\delta_a$	Aileron Deflection
$\alpha$	Angle of attack
$I_{xx}$	Moment of Inertia about x-axis
$I_{yy}$	Moment of Inertia about y-axis
$I_{zz}$	Moment of Inertia about z-axis



## THE A-TEAM

<b>MEMBER</b>	<b>AIAA #</b>	<b>SIGNATURE</b>
Chris Valeski	247255	_____
John Zimmer	281711	_____
Matt Stahr	274283	_____
Mat Thompson	280526	_____
Ryan Wagner	281712	_____
Pat Wongwian	266091	_____
Juan-Carlos Ugarte	280998	_____
Stephanie Bridgeman	281714	_____
Paul Goodwin	281821	_____
Thomas Steva	281938	_____
 <b>FACULTY ADVISOR</b>		
Dr. William H. Mason		_____

# **1. PRELIMINARY DESIGN**

## **1.1 INTRODUCTION**

With the additional need for mobile tactical vehicle support in battle areas, the American Institute of Aeronautics and Astronautics (AIAA) has set forth a Request for Proposal (RFP) for an Inter-Theatre Tactical Transport with Austere STOL Capability. The main purpose of this aircraft is to deliver a Future Deployable Armored Vehicle to areas in which there is not a dedicated airfield. The transport is also required to cruise at commercial aircraft altitudes and speeds and to be deployed from the continental United States. These specific size and cruise requirements are what set this aircraft apart from others. Most larger transport aircrafts have these higher cruise characteristics, yet do not contain the STOL characteristics that are needed for this design. In comparison, smaller transport aircrafts that contain the required STOL characteristics are not capable of reaching the necessary cruise altitudes and speeds.

### **1.1.1 DESIGN REQUIREMENTS**

The requirements set forth by the RFP for this design are what set this aircraft apart from other current military and STOL transports. Aside from the flight requirements, there are also two missions which the aircraft must be able to complete. The first is a transonic ferry mission and the second is a design mission, which includes the transportation and delivery of the Future Deployable Armored Vehicle. The following table, (Table 1.1) outlines the design requirements set forth by the RFP from the AIAA.

Table 1.1 - RFP Requirements

	<b>FDAV Mission</b>	<b>Transonic Ferry</b>
<b>Weight</b>	30 tons	10 tons
<b>Volume</b>	572" x 140" x 114"	1000 cu. Ft.
<b>Takeoff / Landing</b>	2500 ft (balanced field)	2500 ft. (balanced field)
<b>Cruise M</b>	0.8 (min)	0.8 (min)
<b>Cruise Altitude</b>	30,000 ft. (min)	30,000 ft. (min)
<b>Range</b>	500 nm	3200 ft.
<b>Loiter Time</b>	0 min.	45 min.

### 1.1.2 REQUIRED MISSIONS

The AIAA has set forth two missions that the designed aircraft is required to complete. The first is the design mission (Figure 1.1), which involves the delivery of the Future Deployable Armored Vehicle. This mission instructs that the aircraft carry 30 tons of cargo, takeoff off from a runway with a balanced field length of 2500 feet, climb out to best cruise altitude, and travel at Mach 0.8 or larger. Once at this position, the aircraft must cruise for 500 nm, descend to 1000 feet, travel at Mach 0.6, and land on a runway with a balanced field length of 2500 feet. It must then deliver the cargo and mirror the mission without the added weight of the cargo.

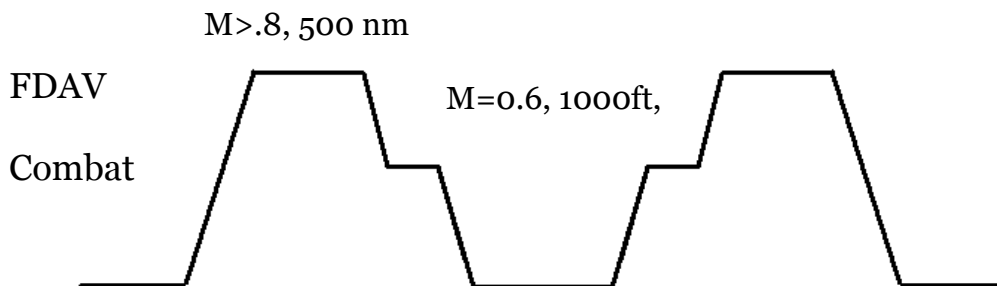
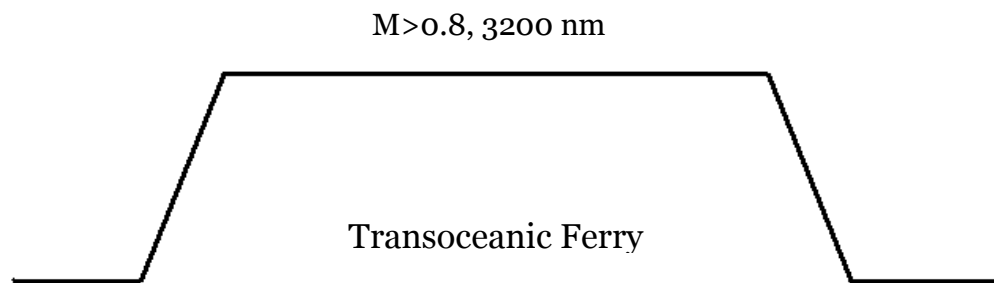


Figure 1.1 – FDAV Combat Mission Profile

The second mission (Figure 1.2) requires the delivery of 10 tons of cargo with a density of 20 lb/cu. ft., and takeoff from a runway of 2500 feet. It must then climb to best cruise altitude and travel at Mach 0.8 for 3200 miles less than the climb distance traveled. The aircraft must then land on a runway with a balanced field length of 2500 ft, but also have the ability to loiter for 45 minutes/150 nautical miles if an approach is missed.



*Figure 1.2 – Transoceanic Ferry Mission Profile*

## 1.2 CONFIGURATIONS

During the preliminary design process there were many different designs considered. Original designs were based off current transport aircraft with design specific modifications. Some of these designs, however, were almost immediately eliminated due to impracticality. After design choices were narrowed down, we carefully considered what the most important aspects of the design should be. We decide that acceptable designs should concentrate on solutions to high cruise speeds and altitudes, extremely short run way distances, ability to land on inhospitable landing strips, and capability to carry the two different payloads.

### 1.2.1 CONSIDERED CONFIGURATIONS

After analysis, the following three main design configurations were considered.

1. High wing, conventional tail, 4 low mounted engines (Figure 1.3)
2. High wing, T-tail, 2 low mounted engines (Figure 1.4)
3. High wing, T-tail, 3 High mounted engines (Figure 1.5)

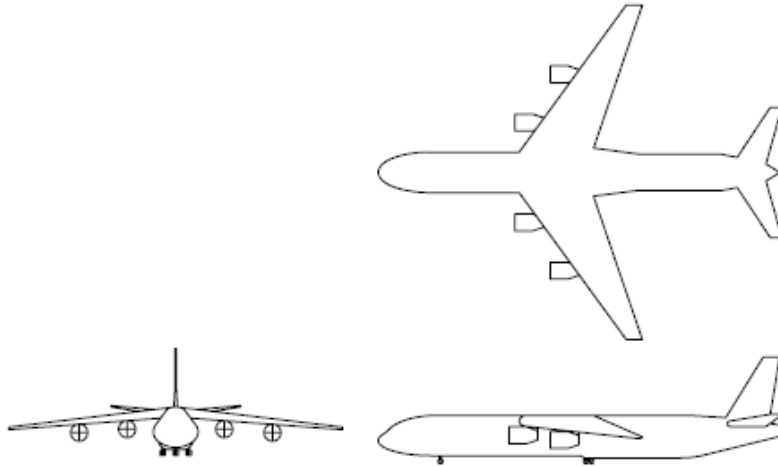


*Figure 1.3 – High wing, conventional tail, 4 low-mounted engines*

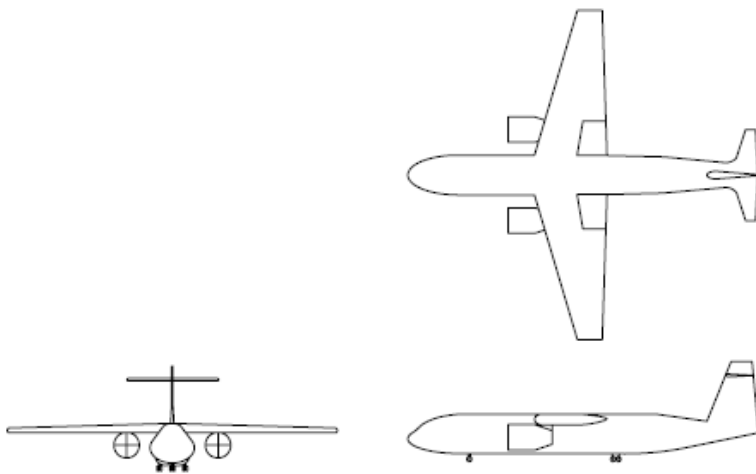


*Figure 1.4 – High wing, T-Tail, 2 low-mounted engines*

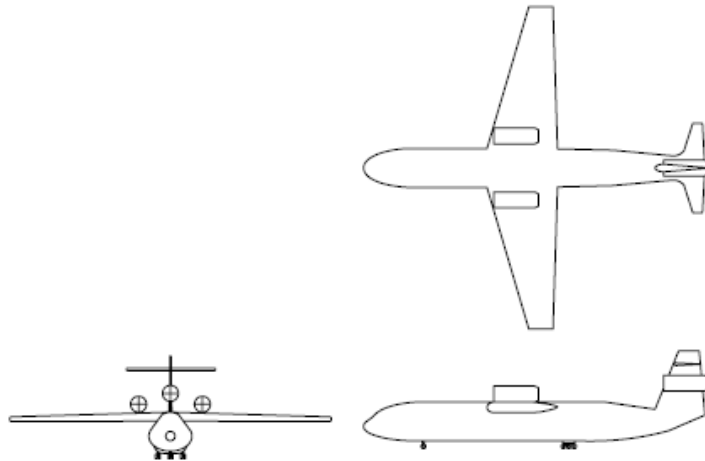


*Figure 1.5 – High wing, T-Tail, 3 high-mounted engines*

The third design was immediately eliminated due to many factors that did not require calculations. At the time, we thought that a power lift system would be needed on the aircraft to produce a coefficient of lift necessary for short take-off distances. The first problem with the third design was that the high-mounted engines would make it nearly impossible for a powered high lift system. Also, servicing high-mounted engines is more difficult than servicing low-mounted engines. Finally the third engine, mounted on the center of the wing, would only supply forward thrust, which is not as critical to our design missions as thrust applied to powered lift. For these reasons, the third design was eliminated first.

The first and second designs were selected to receive further analysis to determine which would best suit the design missions. Historically, the conventional and T-tail designs have been used for similar aircraft; therefore, they caused no obvious concerns for elimination. The positive attributes of these designs are based on ease of maintenance and ability to produce high coefficients of lift for aircrafts with STOL capabilities.

### 1.3 COMPARABLE AIRCRAFT

During sizing, the conventional tail and T-tail crafts were compared to similar aircraft to ensure that sizing numbers were legitimate.

Table 1.2 – Comparable Aircraft Chart

	<b>C-130</b>	<b>C-17</b>	<b>Conventional Tail</b>	<b>T-Tail</b>
<b>TOGW</b>	164,000 lbs	585,000 lbs	216,200 lbs	223,000 lbs
<b>Take-off Distance</b>	3,050 ft	7,740 ft	1,990 ft	1,744 ft
<b>Aspect Ratio</b>	10.1	7.165	7.5	7.5
<b>Wing Area</b>	1,745 ft <sup>2</sup>	3,800 ft <sup>2</sup>	2,340 ft <sup>2</sup>	2,530 ft <sup>2</sup>
<b>High Lift Systems</b>	Lockheed-Fowler type	External Blowing	External Blowing	External Blowing

The conventional tail and T-tail resembled other similar aircraft in most aspects with the exception of a shorter take-off distance (Table 1.2). Its shorter take-off and higher aspect ratio are a result of the aircrafts’ high lift designs.

### 1.4 DESIGN STRATEGY

With the wide variety of military transport aircraft in service today, design measurements and data can easily be generated from aircraft similar to our STOL transport design. The C-17 Globemaster is a current aircraft that has a similar configuration to that selected for our transport. However, a few differences between the two include the cruise altitudes, cruise speeds, size, and landing and take-off distance. Although these are major differences, which are key contributors

to determining the size of the aircraft, figures from comparable aircrafts are useful resources in understanding the sizing process for our design configuration.

## 1.5 FINAL SELECTION

As we previously eliminated the third design, we continued to consider the two first designs to determine which was the most practical. The first two designs were very similar in the fact that they both were high wing and the engines were mounted under the wing. The major differences were the number of engines and the tail configuration. For the weight and size of this aircraft we determined that two engines would provide sufficient power to the aircraft and four was unnecessary. Although these two engines would need to be larger, they are also engines that are comparable in size to engines being used in the military’s fleet of aircraft today. The tail design was finally selected as the T-tail configuration. This decision was based off of current designs, and the ability for the tail control surface areas to be out of the path of the engine thrust, making them more useful in flight. Based on these decision we chose the second option, with a T-tail and two under the wing mounted engines.

*Table 1.3 – Design Evaluation Matrix*

	<b>T-Tail</b>	<b>Low-Tail</b>	<b>3 Engines</b>
<b>Maintainability</b>	<b>+1</b> (easy engine access)	<b>+1</b> (easy engine access)	<b>-2</b> (difficult engine design)
<b>Drag Characteristics</b>	<b>+1</b> (smaller VH, less drag)	<b>-1</b> (drag due to horizontal tail, large VH)	<b>-1</b> (drag due to engine locations)
<b>Handling Qualities</b>	<b>+1</b> (avoids engine)	<b>-1</b> (engine wash over)	<b>-2</b> (nose down moment)

	wash)	horizontal tail)	due to engines/T-tail)
<b>Landing Qualities</b>	<b>+1</b> (engines above ground)	<b>+1</b> (engines above ground)	<b>+2</b> (engines high above ground)
<b>Comfort</b>	<b>-1</b> (engines near fuselage, vibration/noise)	<b>+1</b> (engines further out on wing)	<b>-1</b> (engine on tail, vibration/noise)
<b>Marketability</b>	<b>+1</b> (accepted design)	<b>+1</b> (accepted design)	<b>-1</b> (more radical design)
<b>TOTAL</b>	<b>+4</b> (most practical design)	<b>+2</b>	<b>-5</b>

## 2. CONFIGURATION

The ribs on the wing are placed at about 10% aft of the leading edge to 60%. The ribs on the horizontal tail are placed at about 10% aft of the leading edge to 65%. The ribs are placed every 2.5 ft supported with two spars on each side at the 10% and 65% distance along the wing.

The structure of the fuselage is composed of a pressure cap (solid hemisphere) on the front of the fuselage, six bulkheads of about the same size, two smaller bulkheads on the tail, and the aft pressure cap. Two of the six bulkheads which are along the wing are twice thicker than the other four to support the wing.

The door is designed for the FDAV so it could fit without having to hit the tail of the aircraft and the ceiling inside the aircraft when on the ramp. So it wouldn't hit the ceiling the fuselage cross section was designed to be an oval, diameter distance greater on the vertical than horizontal. It will fit completely inside with an additional 12 inch wide escape path around the vehicle.

The wing has a 28 degrees back sweep and is anhedral to -3 degrees. The horizontal tail has a 27 degrees back sweep. The vertical tail has a 35 degree back sweep it has a 74 ft height from the top of the fuselage.

Flap track fairings are located on the underside of the wings and offer protection for the flap control mechanism as well as improved aerodynamic stability. Two flap track fairings are placed on each wing one at 15.84 ft from the root and the other at 30.4 ft from the root. Wing tips also improve the aerodynamics; they add 8.85 ft of the wing span on each side to a total wing span of 137.7 feet.

Two engines are placed, one on each wing. They are located on pylons ahead of and below the wing leading edges 21.6 ft away from the center of the fuselage to the center of the engines.

### 3. WEIGHT AND BALANCE

#### 3.1 CONSTRAINT DIAGRAM

The constraint diagram was constructed based on the range of capability from RFP and FAR 25 to determine the best W/S and T/W. The square space is the optimal design of W/S and T/W. The constraints for the design are: take-off balance field length of 2500 feet at sea level on a hot day, cruise speed of 471 knots at 30,000 feet, stall speed of 70 knots, climb gradient of 2.4 percent for engine out. The optimal design of T/W vs. W/S is about 0.35 and 85, below is the plot of the constraint diagram.

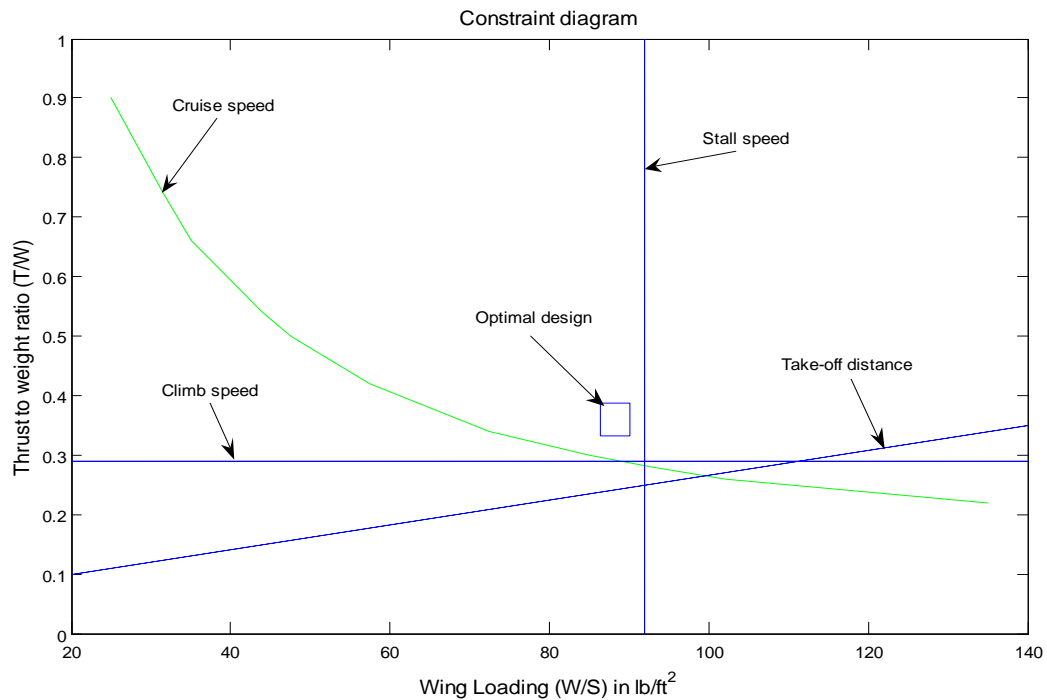


Figure 3.1 – Constraint Diagram

## 3.2 SIZING

Initial sizing of each of our aircraft options were computed by the team member who submitted the design. Weight estimates were extremely crude and were based mainly on Raymer's method. The takeoff gross weights ranged from 168,000 lbs for the conventional tail to 278,000 lbs for the T-tail design. These weights were grossly out of proportion because the only major difference in these two models was the tail configuration. Nikoli's sizing method was used to recalculate these weights and values of 153,000 lbs for the conventional tail and 159,000 lbs for the T-tail. These values seemed too light; however, the 110,000 lbs disparity between the two aircraft was closed.

In order to get a rough estimate of each system in the aircraft we used Raymer's method as given in the text. The values for the systems were only calculated for one aircraft with dimensions averaged between the two aircraft. The reason for this was to get a basic idea of component weights before the aircraft dimensions were finalized. Since these two aircraft are made to accomplish the same mission, the final dimensions would be nearly identical besides the tails. Estimates for weights of fuselage, tail, landing gear, wings, fuel systems, and control systems were calculated. These values gave us a more thorough understanding of why our aircraft weighed as much as it did.

These initial system weights were used as ballpark estimates when we further analyzed each aircraft by means of the Advanced Aircraft Analysis v3.1. This program uses the Raymer method as well, so our values should have been very similar. As can be seen in Fig, the initial estimates of each system differ from the AAA software values by a factor of about 1.4. This makes sense because the takeoff gross weight of the initial estimate was about 1.4 times less than

that of the software program. The weights are higher for the two aircraft because many more systems were taken into account for their two weights.

*Table 3.1 - System Weights \*Using AAA software*

<b>Component</b>	<b>Initial Estimate (lbs)</b>	<b>Conventional Tail* (lbs)</b>	<b>T-Tail* (lbs)</b>
Fuselage	20,700	26,457	21,981
Wing	16,273	22,273	22,644
Empennage	2,340	4,070	5,523
Landing Gear	5,460	7,801	8,615
Nacelle	N/A	2,826	3,755
Structure	N/A	63,249	62,520
Power plant	N/A	17,299	16,458
Fixed Equipment	10,427	12,550	27,725
Empty Weight	62,400	93,278	106,705
<b>TOGW</b>	<b>154,000</b>	<b>216,300</b>	<b>223,200</b>

These final weight values are slightly misleading because these was much more time taken in the computation of the T-Tail design. With more inputs put into the formula for the T-Tail, the weight values jumped up more than the conventional tail design. The conventional tail was also grossly undersized for what is necessary to control an aircraft of this size. The horizontal tail of the conventional design should have been larger than that of the T-tail because the conventional tail has to deal with engine wash running over the elevator. This turbulent flow reduces the rudder's effectiveness and more control surface is necessary to produce the same pitching moment.

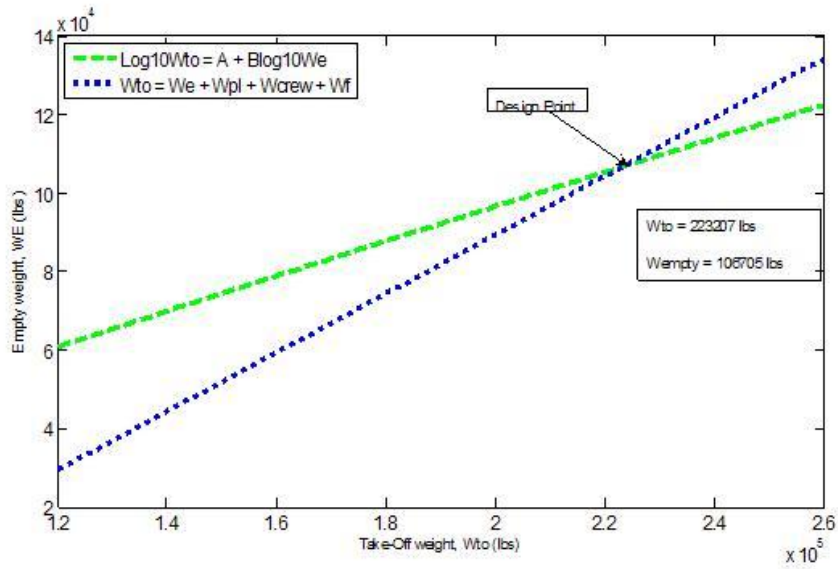


Figure 3.2 - T-tail WE vs. TOGW

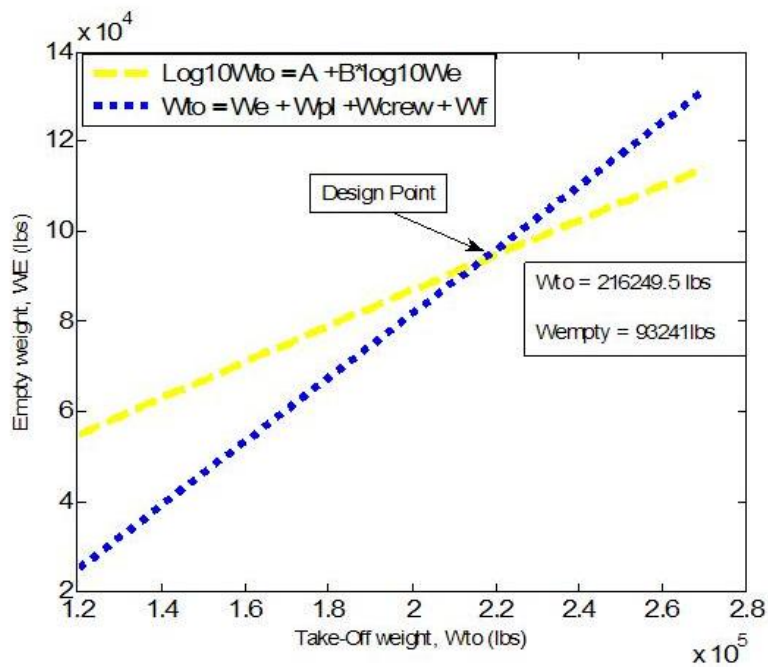


Figure 3.3 - Conventional Tail WE vs. TOGW

After the weight was determined, the AAA program was used to find the optimal design of W/S vs. T/W at  $C_{L_{max}}$  take-off and landing and sea level static thrust available based on initial constraints. The is optimal at W/S of  $88.24 \text{ lb/ft}^2$ , T/W of 0.36,  $C_{L_{maxTo}}$  of 4.75 and sea level static thrust available of 81243 lbs (Figure 3.4).

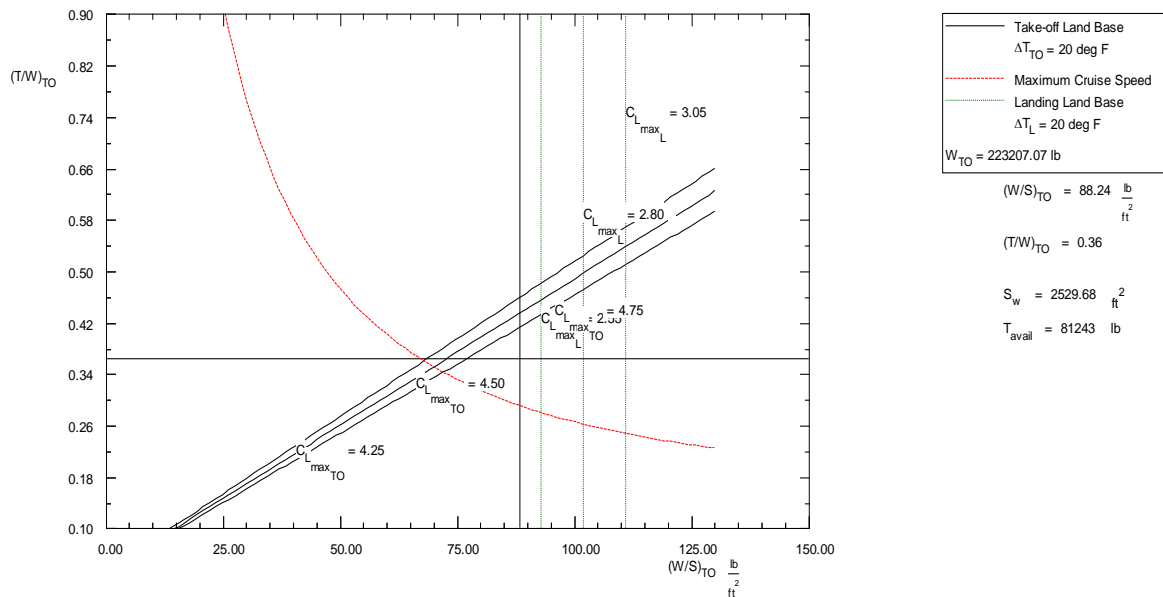


Figure 3.4 - Optimal Design of W/S vs. T/W at  $C_{L_{max}}$

### 3.3 WEIGHT BREAKDOWN OF MR. T

Initial weight estimates were completed using the Raymer method for aircraft sizing. These weights were made more precise by the use of the AAA software which uses the Roskim method for weight sizing. This program allowed us to find not just overall weights, but particular system weights as well. Certain weights, such as the engines and payload were given by factory and RFP specifications, respectively.

Table 3.2 - Weight Breakdown of Mr. T

	<b>Components</b>	<b>FDAV mission (lbs)</b>	<b>Transonic Ferry mission (lbs)</b>	<b>X-cg (ft)</b>	<b>Y-cg (ft)</b>
<b>Structures</b>					
<b>1</b>	<b>Wing</b>	22644.9	22644.9	50.67	13.85
<b>2</b>	<b>Horizontal tail</b>	2768.2	2768.2	125.31	35.03
<b>3</b>	<b>Vertical tail</b>	2765.7	2765.7	115.06	24.78
<b>4</b>	<b>Nacelles</b>	3755.1	3755.1	45.00	15.92
<b>5</b>	<b>Fuselage</b>	21981.3	21981.3	54.83	8.03
<b>6</b>	<b>Main landing gear</b>	6031.6	6031.6	58.56	1.52
<b>7</b>	<b>Nose landing gear</b>	2583.4	2583.4	16.34	1.66
<b>Equipment</b>					
<b>8</b>	<b>Flight controls</b>	880.2	880.2	78.37	11.08
<b>9</b>	<b>APU</b>	1500.0	1500.0	113.53	12.46
<b>10</b>	<b>Instruments systems</b>	200.0	200.0	12.53	11.08
<b>11</b>	<b>Hydraulics</b>	312.2	312.2	67.42	13.85
<b>12</b>	<b>Electrical systems</b>	200.3	200.3	57.60	11.08
<b>13</b>	<b>Avionics</b>	1800.5	1800.5	12.46	6.15
<b>14</b>	<b>Furnishings</b>	3460.0	3460.0	58.15	7.20
<b>15</b>	<b>Air conditioning</b>	940.0	940.0	97.61	6.92
<b>16</b>	<b>Anti-icing</b>	300.0	300.0	96.67	6.92
<b>17</b>	<b>Cargo system</b>	1200.0	1200.0	74.76	6.37
<b>18</b>	<b>Handling gear</b>	50.0	50.0	58.56	6.45
<b>19</b>	<b>In-flight refueling system</b>	329.3	329.3	28.52	14.54
<b>20</b>	<b>Counter measurement system</b>	550.0	550.0	113.95	5.96
<b>21</b>	<b>Radar system</b>	625.7	625.7	5.54	6.75
<b>Propulsion</b>					
<b>22</b>	<b>Engines(2)-installed</b>	14600.0	14600.0	45.0	15.92
<b>23</b>	<b>Fuel system/tank</b>	2064.6	2064.6	48.23	13.85
<b>24</b>	<b>Propulsion system</b>	406.9	406.9	48.23	11.08
<b>Load</b>					

<b>25</b>	<b>Pilots(2)</b>	500.0	500.0	10.38	8.03
<b>26</b>	<b>Crew(1)</b>	250.0	250.0	23.26	8.03
<b>27</b>	<b>Mission Fuel-usable</b>	56495.5	56495.5	58.84	14.26
<b>28</b>	<b>Fuel-trapped</b>	3606.2	3606.2	58.84	14.26
<b>29</b>	<b>Cargo/payload</b>	60000.0	21667.7	49.29	8.03
		<b>223,000</b>	<b>185,668</b>	<b>53.36</b>	<b>15.76</b>

Primary moments of inertia were calculated using the Raymer method. These moment of inertia estimates were defined further once the drawing was completed in the CAD drawing and final length measurements were known.

*Table 3.3 - Moments of Inertia of Mr. T*

$I_{xx}$	$I_{yy}$	$I_{zz}$
1787744 slug-ft <sup>2</sup>	3633483 slug-ft <sup>2</sup>	6441052 slug-ft <sup>2</sup>

### **3.4 FUEL WEIGHT ANALYSIS**

The different segments of the mission consume different amounts of fuel and as fuel is consumed the weight drops, nearly 62,000 lbs as can be seen in Figure 3.4. This can create a large shift in center of gravity if the fuel tanks are not positioned correctly. Fuel weights play a key role in finding the design point. The design point is a point on the graph of takeoff gross weight vs. empty weight. As the two weights increase, the empty weight required line crosses with the empty weight required line, the location where these two points cross is known as the design point. This point gives you the values for optimal takeoff gross weight and empty weight.

Table 3.4 - Mission Profile Table for T-Tail

		<b>W<sub>begin</sub> lb</b>	<b>ΔW<sub>Fused</sub> lb</b>	<b>W<sub>Fbegin</sub> lb</b>
1	Warm-up	216249.5	2162.5	61707.3
2	Taxi	214087.0	2140.9	59544.8
3	Take-off	211946.1	2119.5	57403.9
4	Cruise	209826.7	54038.1	55284.4
5	Land/Taxi	155788.5	1246.3	1246.3

## 4. AERODYNAMICS

### 4.1 GENERAL WING CONFIGURATION FACTORS

The Mr. T features high-mounted wings, which were chosen with the RFP landing requirements in mind. The RFP states that the aircraft design must be able to land on non-ideal landing surfaces i.e. non paved surfaces and the advantage of having high-mounted wings is that it lowers the possibility of a significant amount of dirt and other debris from getting into the engine inlet that would hinder aircraft performance. Research on existing STOL military transport aircraft such as the C-17, C-130, C-27, and An-72 also showed this was the most common wing mounting position (Jane's).

### 4.2 T-TAIL CONFIGURATION

This aircraft design features a T-tail configuration in combination with high-mounted wings. This configuration is common among current STOL military transport aircraft, such as the C-17 and C-27. The main advantage to the T-tail is that the horizontal surface of the tail is kept out of the airflow from the wing, resulting in smoother flow over the tail plane surfaces, more predictable performance characteristics, and improved pitch control. These flight characteristics are important especially for a STOL military transport because these planes are operating at low speeds, where smooth airflow greatly effects control. The prominent disadvantage of the T-tail configuration is the possibility of a deep stall at high angles of attack. This deep stall occurs when the turbulent flow wake over the stalled main wing surface blanks the horizontal T-tail surface, which results in the elevators becoming ineffective and the aircraft not being able to recover

from stall. This problem can be avoided by installing a stick shaker into the T-tail design, which will alert the pilot to the problem before it occurs. Another possible solution to the problem of deep stall was to place the engines further aft in a manner similar to the DC-9 instead of having wing-mounted engines. This idea was ruled out due to the added weight that results from having aft-positioned engines and the overall balance issues that can occur.

### 4.3 WING PLANFORM SELECTION

Based on the gross take-off weight and wing loading calculations made previously and using aspect ratio values determined from historical STOL transport aircraft data, the wing planforms were determined and drawn using the Advanced Aircraft Analysis software. Since the RFP states that the aircraft must cruise at Mach 0.8, the wings were swept to  $28.28^\circ$  to reduce wave drag, which becomes a factor in the transonic Mach range ( $\sim 0.70$  to  $1.2$ ). Wave drag is an added drag component that is present during the transonic region due to the presence of shock waves on the wing surface. A leading edge sweep angle of  $28.28^\circ$  was determined based off a desired cruise Mach speed of 0.82 using historical aircraft cruise data (Raymer). The wing planform for the Mr. T appears in the Figure 4.1 below and a table of wing parameters appears in Table 4.1.

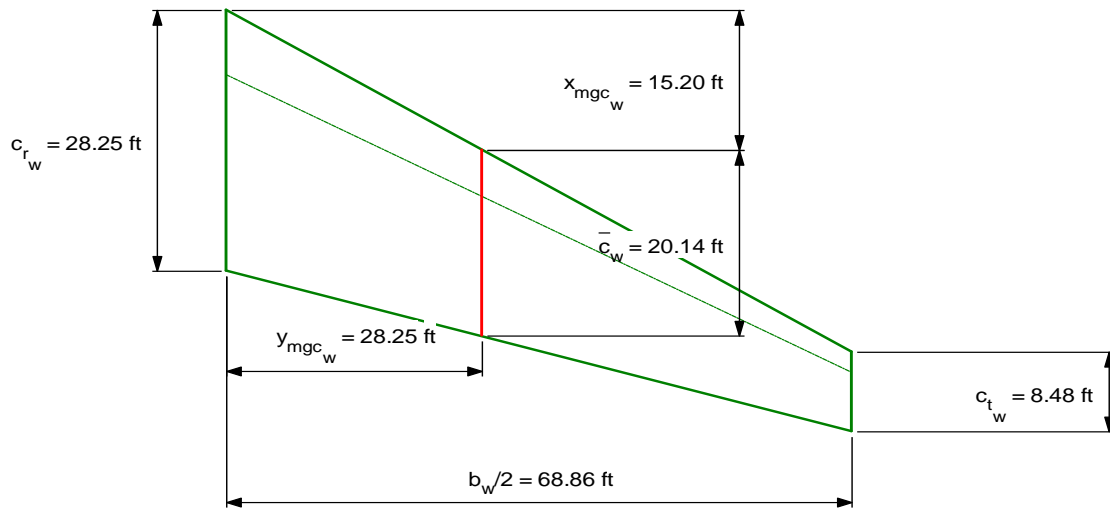


Figure 4.1 - Wing Planform Area, T-tail Aircraft

Table 4.1 - Wing Geometry, T-tail Aircraft

<b>Wing Aspect Ratio</b>	7.5
<b>Total wing Area</b>	2576 ft <sup>2</sup>
<b>Wing Span</b>	137.72 ft
<b>Wing LE Sweep</b>	28.28
<b>Wing TE Sweep</b>	14.09
<b>Wing TaperRatio</b>	0.3
<b>Wing Quarter Sweep</b>	25
<b>Wing Root Chord</b>	28.25 ft
<b>Wing Tip Chord</b>	8.48 ft
<b>Wing MGC</b>	20.14
<b>Wing MGCy Distance</b>	28.25
<b>WingNmgc</b>	15.2

## 4.4 TWIST DISTRIBUTION

To reduce cruise drag and improve aerodynamic efficiency at cruise, the optimal twist distribution for the wing was determined and implemented. This was determined using the LamDes wing twist code (Mason), which uses the wing planform to calculate optimal twist. The wing twist distribution appears as Figure 4.2. The addition of wing twist will result in a beneficial positive nose up pitching moment.

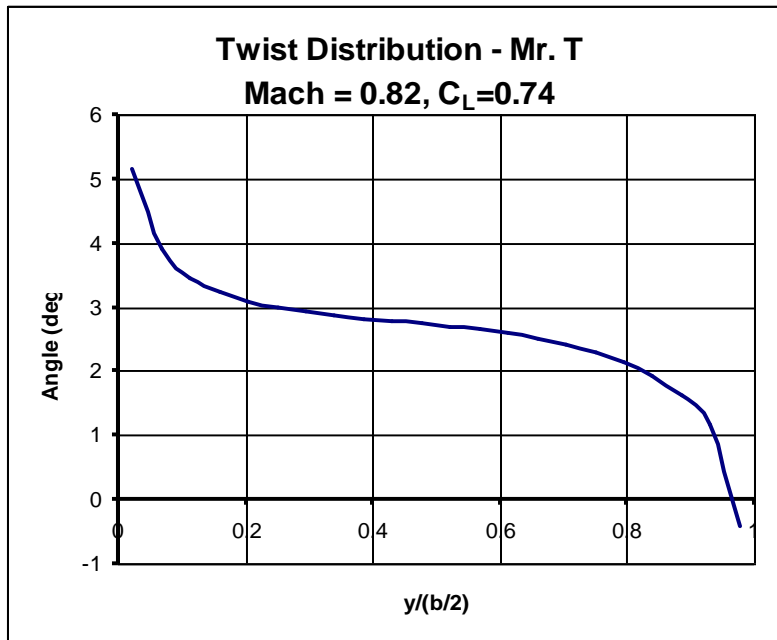
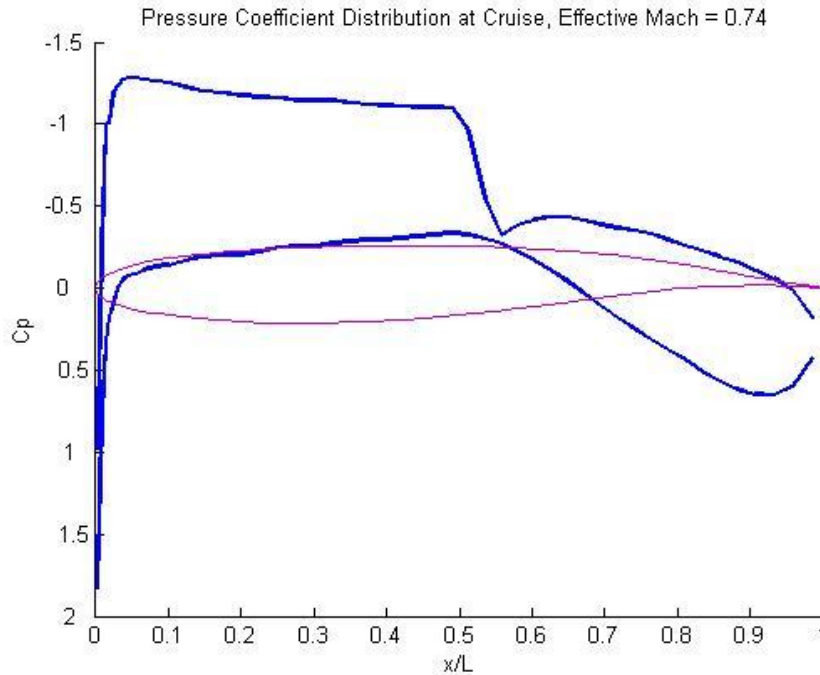


Figure 4.2 - Mr. T Wing Twist Distribution

## 4.5 AIRFOIL SELECTION

The mission requirements in the RFP state that the STOL transport aircraft must have a cruise Mach speed of at least 0.8. This Mach value falls within the transonic speed range of 0.7 to 1.2, which significantly affects the airfoil selection process (Mason). This cruise Mach speed is particularly high for a STOL jet transport aircraft. The major issue

to be considered at transonic speeds is the presence of a shock wave over the upper surface of the wing due to local supersonic flow regions. This shock wave results in the emergence of wave drag over the wing surface. As a result of these flow issues, the aerodynamics team made the decision to test different supercritical airfoil shapes in order to better control and soften the adverse shock wave effects that appear at the required cruise speed. The thickness per chord length ( $t/c$ ) needed for the wing had been previously determined to be 12% based on desired cruise Mach speed and  $t/c$  values used on the reference aircraft. It was also determined that the ideal shock wave location for aerodynamic efficiency would be about 60% chord length. Several NASA supercritical airfoils were analyzed by running the TSFOIL code at angles of attack of  $0^\circ$ ,  $0.5^\circ$ , and  $1^\circ$  with effective Mach values of 0.70, 0.72, and 0.74. Based on this airfoil analysis, the NASA SC-24012 gave the best results with regard to shock location and strength with an effective Mach value of 0.74. The quarter chord angle was used to convert the effective Mach speed and this resulted in a  $M_{\text{cruise}}$  value equal to at 0.82 Mach, which satisfies the cruise speed requirement. This airfoil analysis also determined  $C_D$  due to wave drag to equal 0.02655. The pressure coefficient distribution appears as Figure 4.3.



*Figure 4.3 –  $C_p$  Distribution at Cruise*

The other major consideration in the airfoil selection process, in addition to the cruise performance, was the field performance and obtaining the  $C_L$  necessary to achieve the given mission goals. The supercritical airfoil selected generated higher lift than subsonic airfoils with its larger leading edge radius and the high aft camber. In addition, the aft camber helps to weaken the normal shock. The aircraft's high lift system will be discussed in detail later in this report, but the airfoil analysis for cruise yielded a  $C_L$  value of 0.744.

## 4.6 FRICTION AND FORM DRAG

The friction drag for the aircraft was needed in order to determine the drag polar plot at the cruise condition. This was done using the FRICTION code, which determines the friction and form drag of the aircraft (Mason). The input parameters for this code are the wetted area, reference length, and thickness/chord (t/c) or distance/length (d/l) depending on the whether the surface was planar or a body of rotation for each of the major structural components. The output for the FRICTION code appears in Table 3.2.  $C_{Dfriction}$  was determined to equal 0.0169 and  $C_{Dform}$  was equal to 0.0047.

Table 4.2 - Friction and Form Drag Calculations

COMPONENT	$C_F$	$C_F * S_{WET}$	$C_F * S_{WET} * F_F$	$CD_{COMP}$
WING	0.00227	0.34446	0.46321	0.00015
FUSELAGE	0.00176	0.62182	0.65971	0.00021
VERTICAL TAIL	0.00210	2.09145	2.67706	0.00086
HORIZ TAIL	0.00229	1.27355	1.44628	0.00047
ENGINES	0.00259	0.52833	0.96551	0.00031
WINGLETS	0.00257	0.40143	0.51243	0.00017
SUM		5.26105	6.72420	0.00217

REYNOLDS NO./FT = 0.192E+07 Altitude = 35000.00 XME = 0.820

FRICTION DRAG: CDF = 0.0169

FORM DRAG: CDFORM = 0.0047

## 4.7 DRAG POLARS AT CRUISE

Using the friction drag and wave drag that were determined previously, the drag polars were able to be plotted for the cruise flight condition. The resulting drag polar plot for the untrimmed condition were compared with drag polar plots from NASA data for

trimmed and untrimmed conditions in order to determine the amount of drag that would be added by trimming the Mr. T. Both of these drag polar plots appear as Figures 4.4 and 4.5. Given that the cruise  $C_L$  was calculated to equal 0.744, the  $C_{D_{cruise}}$  for the untrimmed condition is equal to 0.025 and roughly 0.026 for the trimmed condition. These points appear on both figures.

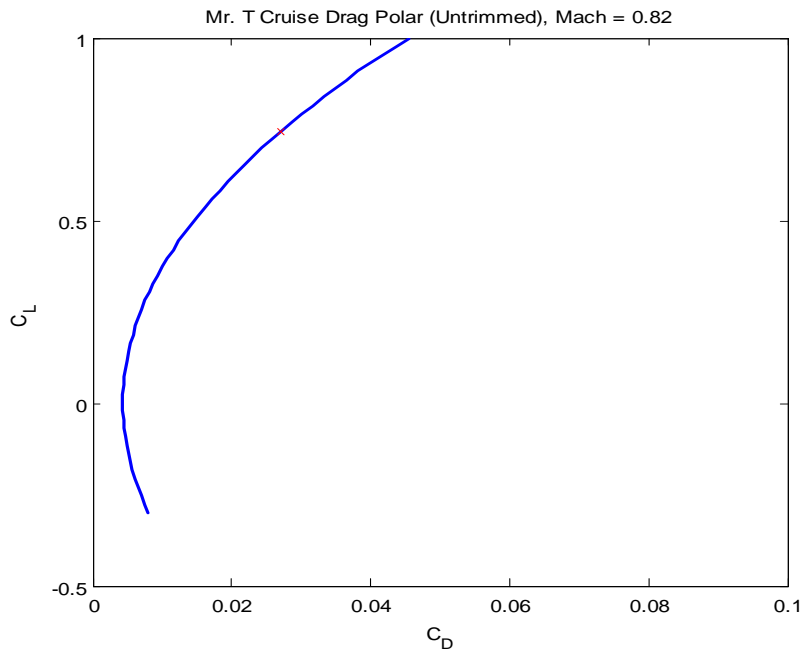


Figure 4.4 - Drag polar for the Untrimmed Cruise Condition

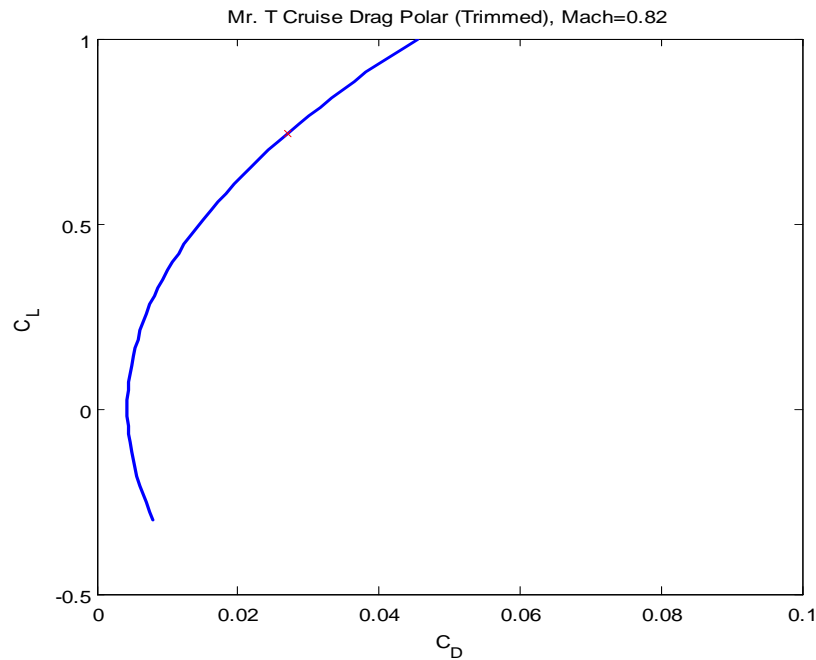


Figure 4.5 - Drag polar for the Trimmed Cruise Condition

## 4.8 CRUISE DRAG

Cruise drag was determined to be 13,500 lbs. This value was initially estimated to be a much higher value of 20,601 lbs., but this value was approximate and the newer value has higher accuracy.

## 4.9 COEFFICIENT OF LIFT AT TAKE-OFF

As a STOL aircraft, achieving the required take-off distance was one of the main mission drivers. Using the take-off and landing Matlab performance program, a preliminary calculation was made for the required coefficient of lift to achieve the take-off and landing distances given in the RFP. This program was created in order to check that the aircraft would achieve the take-off and landing distances based on a number of

input parameters for the aircraft. Since at this point in the design process many of the other inputs were close to being finalized,  $C_L$  values were the only inputs not determined. The take-off code was used more specifically to find the minimum  $C_L$  required to meet the balanced field length requirement. Initially this value was determined to be 4.6, but was increased to 4.75 after it was estimated that the total gross weight of the aircraft would be higher than originally estimated. This  $C_L$  requirement at take-off reiterated the necessity of using some type of powered high lift system to meet the RFP requirements. Note that the maximum  $C_L$  for mechanical high lift systems is around 3.0.

## 4.10 HIGH LIFT SYSTEMS

Several types of high lift systems were considered including triple-slotted flaps, blown flaps, vectored thrust, and a jet-augmented wing. Out of these, triple-slotted flaps and externally blown flaps were determined to be most practical and were considered in greater detail. Triple-slotted flaps are found on the Boeing 777 and externally blown flaps are used on the C-17; both were used as reference aircraft. Figures 4.6 and 4.7 show diagrams of each lifting system. The triple-slotted flap configuration consists of gaps between the flaps and the wing, which enable high pressure air from below the wing to re-energize the boundary layer over the flap system. This delays stall by helping the airflow stay attached to the series of flaps. The disadvantage of this system is that it has high complexity which could result in more frequent maintenance and repairs. This type of mechanical high lift system was only considered extremely early on in the design process. Once it was determined that a  $C_L$  at take-off of over 3.0 would be required, only powered lift systems were considered. As stated in the previous section, the  $C_{Lmax}$  for

mechanical lift systems are no greater than 3.0 so given that aircraft needed to generate a  $C_L$  of 4.75, externally blown flaps were then analyzed by the design team.



*Figure 4.6 - Triple-slotted flaps*

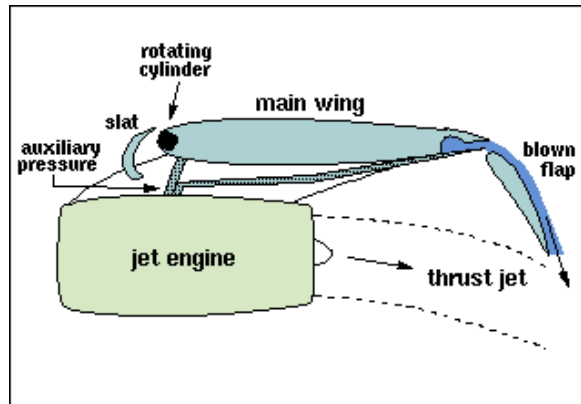


*Figure 4.7 - Externally Blown Flaps*

Externally blown flaps work by diverting some engine exhaust downward which results in more lift. More specifically, engine exhaust from the engines impinges directly on conventional slotted flaps, which are deflected downward to increase total lift. Based on several sources, the addition of externally blown flaps can increase the lift by 85% (Mason). Externally blown flaps enable the aircraft to make slow, steep approaches with heavy cargo and for this reason this high lift system was selected over the triple-slotted

flaps system. Also the group had initially estimated that the  $C_{L_{max}}$  required was closer to 3.0 and this was the reason for considering the triple-slotted flaps. Upon further analysis it was determined that a higher  $C_{L_{max}}$  of 4.75 at take-off was needed. The one trade off that will occur by this selection is that externally blown flaps use some of the thrust from the aircraft engines to generate lift. This will result in the necessity for larger engines to produce the added required thrust and this will increase the entire aircraft weight.

Using external blown flap data from wind tunnel tests performed by NASA, the design team generated a  $C_L$  vs.  $\alpha$  curve for the Mr. T (Campbell). The curve is based off of the aircraft's thrust coefficient ( $C_\mu$ ) which was calculated to equal 1.91. This curve appears in Figure 4.8. The aircraft will take off at an angle of attack in the range of  $7^\circ$  to  $11^\circ$  and according to this figure these alpha values correspond to  $C_L$  values of greater than 4.75, which confirm the externally blown flap system will generate the amount of lift needed for short take-off and landing capabilities. (Figure 4.8)

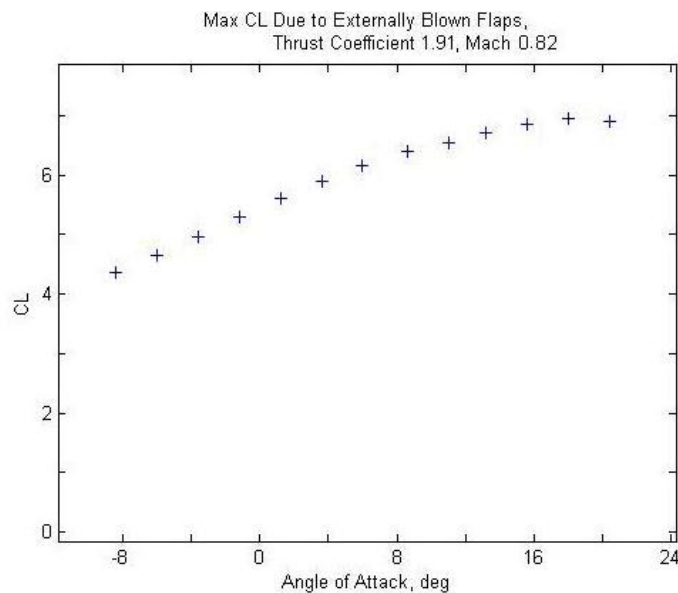


Figure 4.8 -  $C_L$  vs. angle of attack curve for externally blown flaps

## 4.11 LEADING EDGE LIFTING DEVICES

In addition to the externally blown flaps, leading edge flaps were added to the wing design. According to Raymer, these can result in a  $\Delta C_{l,max}$  of 0.3. Leading edge slats improve the flow by “protecting” against flow separation when rapid acceleration occurs around the leading edge. Another wing parameter that was determined was that the high lift system will take 25% of the wing chord length. This means that the ratio between the chordwise length of the elevator and the wing chord length ( $C_e/C$ ) is equal to 0.25. Using Raymer’s initial maximum lift coefficient estimation method, the total lift required to meet take-off and landing distances will be met with the above stated high lift systems. Based on the amount of lift that is produced by the externally blown flap system combined with the addition of leading edge slats, the Mr. T will exceed the  $C_L$  of 4.75, which is required to meet the take-off distance stated in the RFP.

## 4.12 DRAG POLARS FOR TAKE-OFF AND LANDING

### CONDITIONS

Drag polar plots were also created for the take-off and landing conditions. These appear as Figures 4.9 and 4.10 below. These show that at take-off the drag coefficient will approximately equal 1.05 and for the landing condition the drag coefficient will equal 1.2.

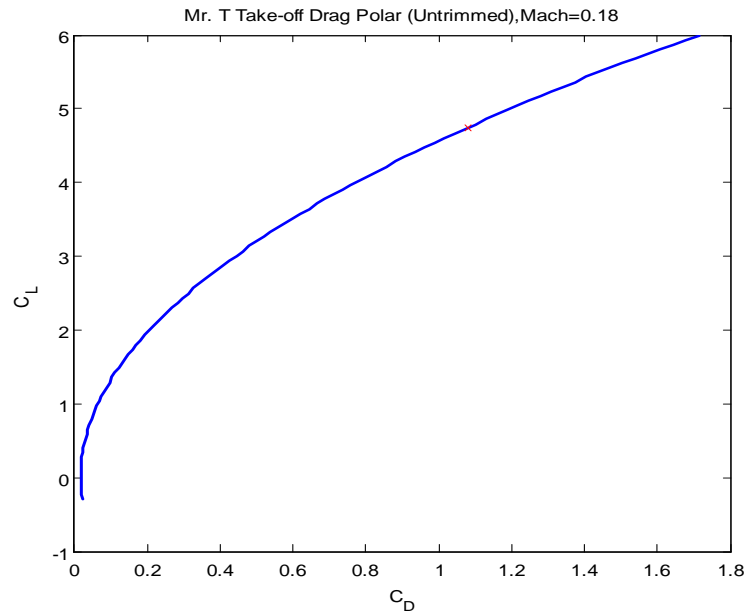


Figure 4.9 - Drag Polar for Take-off

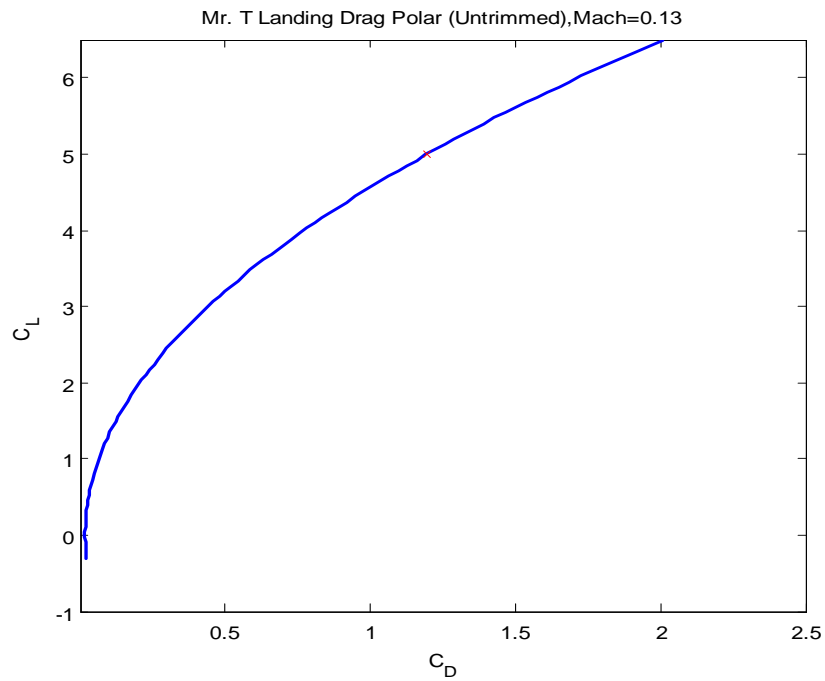


Figure 4.10 - Drag Polar at Landing

## 4.13 EFFECT OF EXTERNALLY BLOWN FLAPS ON PITCHING MOMENT

The pitching moment coefficient vs. the angle of attack in degrees in Figure 4.11 shows a common problem for STOL concept planes. For all angles of attacks, the pitching moment is negative, which means a significant amount of trim is required to maintain a stable slope at cruise. A large tail can help establish the trim needed due to the pitching moment created by the externally blown flaps, and the Mr. T. does have a large tail which helps the pitching moment get closer to zero making a stable slope for the aircraft.

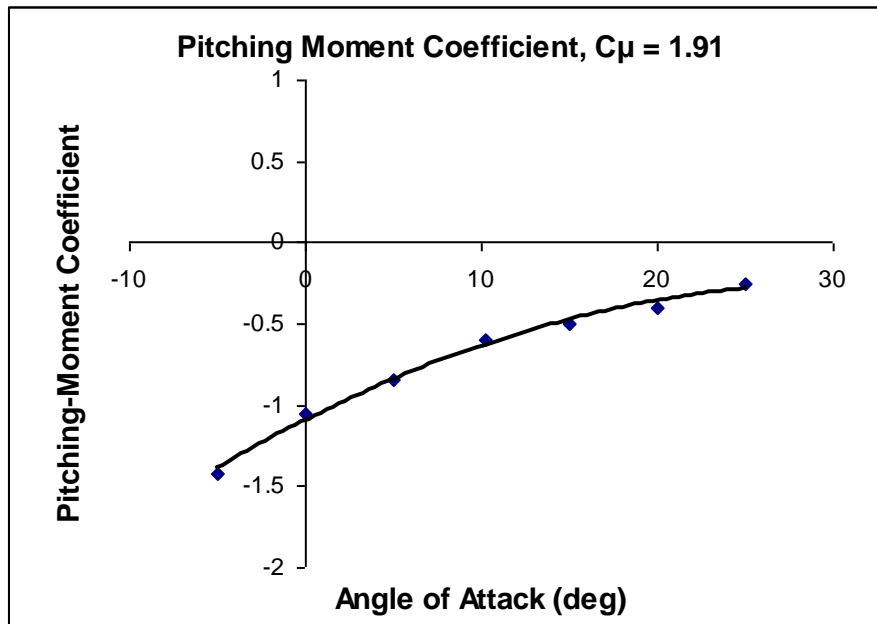


Figure 4.11 – Pitching Moment Coefficient Curve

## 5. PROPULSION

### 5.1 INTRODUCTION

For STOL, the transonic ferry mission, and the design mission, the engine design is a crucial component in meeting these requirements. The engines evaluations were based on safety, performance, reliability, operational cost, and minimal installation penalty. The most critical requirements for the propulsion system are:

1. For transonic ferry mission, balance field length for take-off and landing must not exceed 2,500 feet on a hot day at sea level
2. For design mission, aircraft must be able to fly at least 3200 nautical miles without refueling.
3. Cruise speed of at  $M \geq 0.8$  at 30000 feet.

### 5.2 ENGINE SELECTION

The aircraft will be operated at Mach 0.8; high Bypass ratio engines are needed to maximize the static thrust. We decided to use two engines as opposed to four because two engines are generally more efficient, and therefore cost less per hour of use compared to four engines. The two engine design is also lighter, which lowers the maximum gross take-off weight and reduces complexity in the design. Finally, two engines provide a lower initial cost to the customer. The negative effect of using a two engine design is the analysis needed for engine-out scenarios. With a four engine design, one can balance the thrust in an engine-out scenario, however with a two engine system one cannot. Therefore, two engines will provide a yaw moment that will be analyzed and calculated

in section 5.3 so that flight will be possible if engine-out occurs in this design, since the FAA also required the aircraft to be able fly with an engine out.

Based on Advanced Aircraft Analysis software, the aircraft has a TOGW of 223200 lbs, a thrust to weight of 0.36 with a maximum take-off sea level static thrust of 81245 lbs. This indicates that each engine will need 40622 lbs of sea level static thrust. Listed below in Table 5.1 are the engines with the sea level static thrust range from 40440-53200 lbs.

*Table 5.1 – Engine Comparison*

<b>Engine</b>	<b>To thrust (lb)</b>	<b>Length (in)</b>	<b>Diameter (in)</b>	<b>Weight (lb)</b>	<b>Bypass</b>
AIAA	42046	135	83	8000	6.0
PW4050	52,000	132.7	97	9213	5.1
PW2043	42,600	141.4	78.5	7300	5.3
F117-100	40,440	146.8	84.8	7100	5.9
CF6-50	52,500	173	86.4	8721	4.3
GEEx-10A	53,200	185	111.3	12,439	9.2
RB211-524B	50,000	122.3	85.8	9,814	4.4

Seven engines were chosen for initial analysis based on sea level static thrust requirements. The engines were chosen from three different manufactures: Pratt & Whitney, GE, and Rolls-Royce, AIAA also provided the engine deck with performance data.

After further analysis, F117-100 was found not suitable for this design because the sea level take off thrust is smaller than the thrust require, while GEEx-10A, PW4050,

CF6-50 and RB211-524B give very high sea level take off thrust value; however, they would need to be largely scaled down to meet the thrust requirement. It would reduce the cost to choose the engine that had already been built and was available on the market, than to choose one that would need to be scaled down. This reduced the choice to two engines, AIAA and PW2043. Both engines have very similar sea level take off thrust of 42046 lbs for AIAA, and 42600 for PW2043. However, the PW2043 is 700 lbs lighter. The PW2043 was selected over AIAA engine because of its lighter weight and its fulfillment of the thrust requirements after factoring in thrust losses due to height, installation, and mass bleed. The AIAA engine was provided based on “rubberized engine” which needed to be designed, tested, and built; it would reduce the cost to use the engine that had already been tested, built, and was available on the market.

The PW2043 is rated at 43000 lbs of sea level static thrust with Bypass ratio of 5.1. It is the latest version of the PW2000 family. The engine uses the latest generation of materials and design processes to reduce weight, improve performance, and lower maintenance cost with addition thrust capability at high altitudes and elevated temperatures. The main characteristics of PW2043 are show in Table 5.2 below.

Table 5.2 - PW 2043 Information

Performance		Dimension	
Take off rating (lbs)	43000	Length (in)	141.4
Maximum continuous sea level static thrust (lbs)	36420	Nominal Diameter (in)	78.5
By pass ratio	5.1	Dry Weight (lbs)	7300
Maximum thrust continue at sea level(lbs)	36640		
Fan pressure ratio	1.7		
Overall pressure ratio	5.3		
Sea level static TSFC	0.39		
Sea level static airflow (lb/sec)	1425		

The PW2043 engine is certified for Extended-range Twin-engine Operations (ETOPS), which allow aircraft to fly over water, desert, or remote polar area that were previously off limits to twin engines aircraft. The PW2000's technical innovation provides unequalled performance; the engine was the first to offer Full-Authority Digital Electronic Control (FADEC), an electronic engine control system. The FADEC digitally calculates and precisely controls the fuel flow rate to the engines giving precise thrust, which allows the aircraft to have better fuel efficiency, lower operation maintenance cost, better integration between engine and aircraft system, and reliability. The engine is also equipped with Reduce Temperature Configuration (RTC), this feature provides longer time on the wing, lower maintenance cost, and good environmental performance. PW 2000's family has accumulated over 16 million flying hours through March 2003. Some aircraft that are powered by the PW2000 family include C-17, Boeing 757 and Ilyushin IL-96.

## 5.3 ENGINE PERFORMANCE

Engine performance is dependent on altitude, Mach number, and flight condition. In order to meet each flight condition, engine performance data is needed at each flight envelope; however, PW2043's performance data was unavailable upon request from the manufacture. The analysis was done using Aircraft Engine Design Software. PW2043 has a Bypass ratio 5.1 and a maximum take off sea level static thrust of 43000 lbs with sea level static airflow of 1425 lbs/sec. Figure 3.1 shows the specific fuel consumption (TSFC) as a function of Mach number. At sea level, the airplane has specific fuel consumption of 0.39; specific fuel consumption is increase linearly with Mach number. Figure 3.2 shows the thrust available as a function of Mach number. The take off thrust available at sea level is 43, 000 lbs. At cruise speed at 30,000 feet, the thrust available is about 14,000 lbs. At the higher altitude, the thrust tends to stay constant as the Mach number increases.

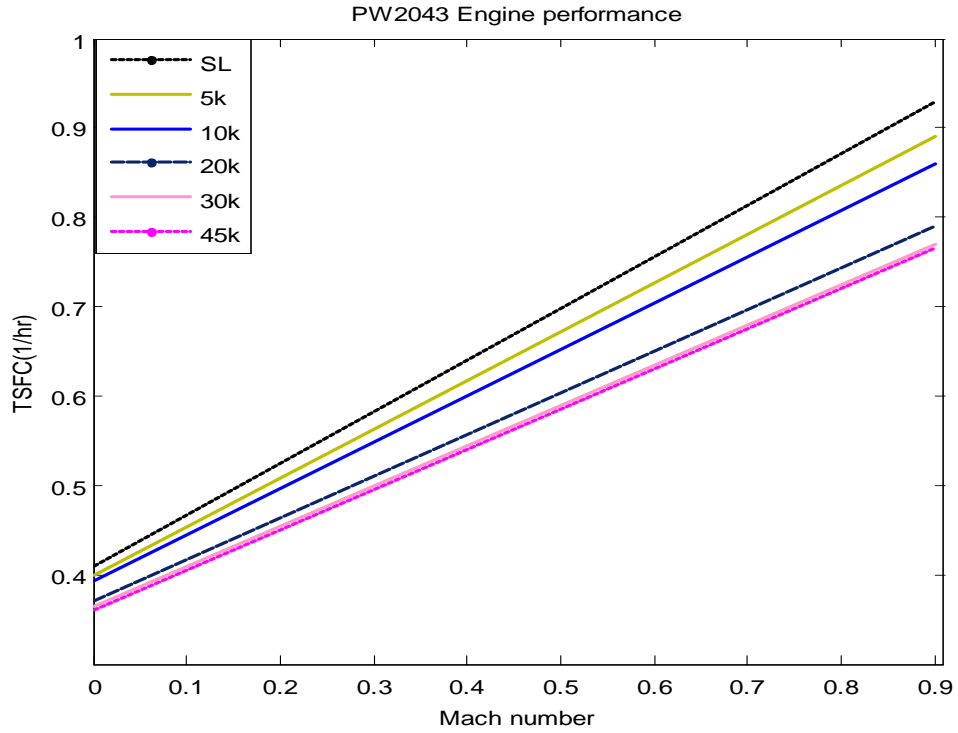


Figure 5.1 – PW2043 Engine Performance

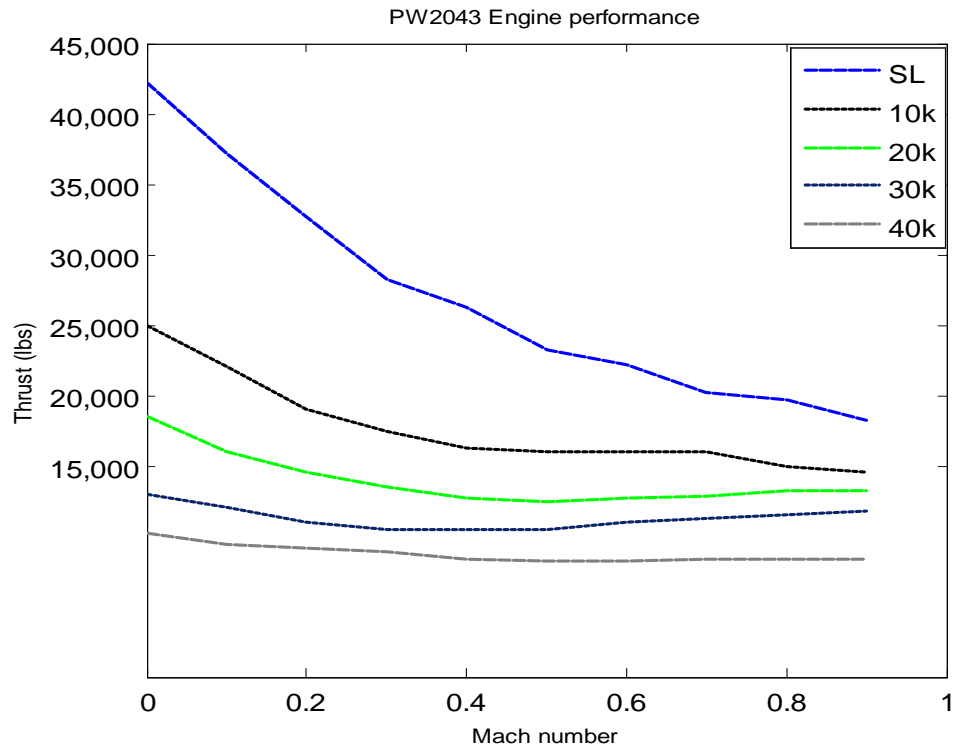


Figure 5.2 – PW2043 Engine Performance

## 5.4 ENGINE OUT

FAR 25 requires the aircraft to be able to fly with an engine out. The calculations in Table 5.3 below show engine out requirements at cruise speed of  $M=0.82$  at 30,000 feet, and climb performance at stand sea level. At the cruise condition, thrust requires is 11485 lbs with the thrust available of 14,500 lbs. The maximum yaw moment ( $N_{TOEI}$ ) occurs at equilibrium flight condition; the calculation was based on FAR 25.149, which allow the bank angle of  $\leq 5^\circ$  with side slip angle of  $2^\circ$ . The plane produced maximum yaw moment ( $N_{TOEI}$ ) of 576,000 ft-lbs. As result, the plane requires the aileron deflection margin ( $\delta_r$ ) of  $15.14^\circ$  with  $5^\circ$  to allow for engine out maneuvering. The aileron is capable of producing a deflection of  $17.5^\circ$ ; this allows the plane to counteract the engine out yaw moment. Note: Take off angle of 8-11 deg to 35ft clearance, climb at 15deg after Table 5.3 lists different engine out scenarios.

Table 5.3 - Engine Out Condition

	One Engine out	One Engine	Two Engine
Cruise at $M = 0.82$ , @ 30,000 ft (Thrust requires)	11485 lbs	14,500 lbs	29,000 lbs
$N_{TOEI}$	576,000 ft-lbs	576,000 ft-lbs	0
$N_{DOEI}$	86400 ft-lbs	86400 ft-lbs	0
$D_{OEI}$	7200 lbs	7200 lbs	7200 lbs
$\delta_r$	$15.14^\circ$	$17.5^\circ$	$17.5^\circ$
<b>Climb</b>			
Velocity Best rate of climb	550 ft/min		4270 ft/min
Maximum angle of climb	$8.5^\circ$		$17.67^\circ$

To meet the climbing requirement, the plane is required to climb at a steady climb rate of  $\geq 300$  feet per minute gradient (FAR 25). After analysis, the plane was able to meet the climb requirements with the best rate of climb of 550 feet per minute at maximum angle of climb of  $8.5^\circ$  for single engine and 4270 feet per minute for two engines at maximum angle of climb at  $17.67^\circ$ . Figure 3.3 shows the climb gradient of the aircraft as the function of air speed. Climb gradient stays very constant as the air speed increases, for engine out condition; climb gradient is about 2.9%, while the two engine condition is about 13%.

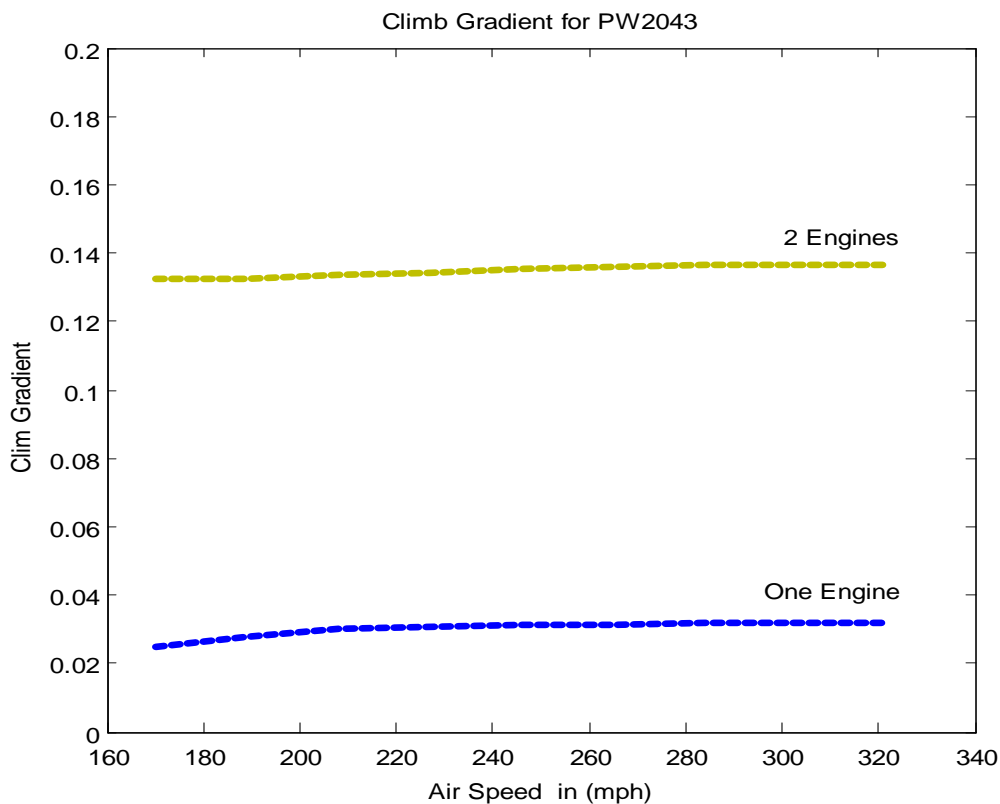


Figure 5.3 – Climb Gradient for PW2043

## 6. STABILITY AND CONTROL

### 6.1 STABILITY AND CONTROL DERIVATIVES

The Mr. T was designed to be slightly statically and dynamically stable, giving it enough stability but still allow maneuverability. This requires that  $C_{L\alpha}$  be less than zero, and  $C_{m\alpha}$  be positive. The stability and control derivatives for the Mr. T were found using the Advanced Aircraft Analysis (AAA) software produced by the DARcorporation. This software uses the Roskim method for stability analysis. The values in were found for straight and level flight at Mach 0.8 at an altitude of 30,000 feet, as well as takeoff and landing at sea level.

*Table 6.1- Stability and Control Values for Mr.T at Flight Conditions*

	<b>Cruise at 30k</b>	<b>Take-off at Sea level</b>	<b>Landing at Sea level</b>
$C_{L\alpha}$	5.55	5.61	5.61
$C_{m\alpha}$	-0.524	-0.314	-0.923
$C_{m\dot{\alpha}}/C_L$	-0.0937	-0.0572	-0.1471
$C_{Lq}$	10.41	10.27	10.59
$C_{mq}$	-13.55	-13.32	-14.29
$C_{L\delta_e}$	0.84	0.84	0.84
$C_{m\delta_i}$	-4.14	-4.03	-4.17
$C_{l\delta_i}$	-0.195	-0.195	-0.195
$C_{n\delta_i}$	-0.00512	-0.00512	-0.00512
$C_{Y\delta_r}$	0.67	0.65	0.70
$C_{l\delta_r}$	-0.0367	-0.0367	-0.0384
$C_{n\delta_r}$	0.125	0.125	0.135
$C_{Y\delta_p}$	-0.646	-0.646	-0.646

$C_{n_\beta}$	0.0947	0.1134	0.1573
$C_{l_\beta}$	-0.0842	-0.0842	-0.0842
$C_{Y_r}$	0.542	0.536	0.524
$C_{n_{\dot{\beta}}}$	-0.00347	-0.00339	-0.00348
$C_{l_{\dot{\beta}}}$	-0.00147	-0.00142	-0.00153
$C_{Y_{\dot{\beta}}}$	0.542	0.539	0.546
$C_{n_{\ddot{\beta}}}$	-0.0106	-0.0106	-0.0106
<b>Static Margin</b>	<b>13.7% MAC</b>	<b>18.3% MAC</b>	<b>8.86% MAC</b>

The following Figure 6.1 shows variation of  $C_m$  with  $C_L$  for three different rudder deflections.

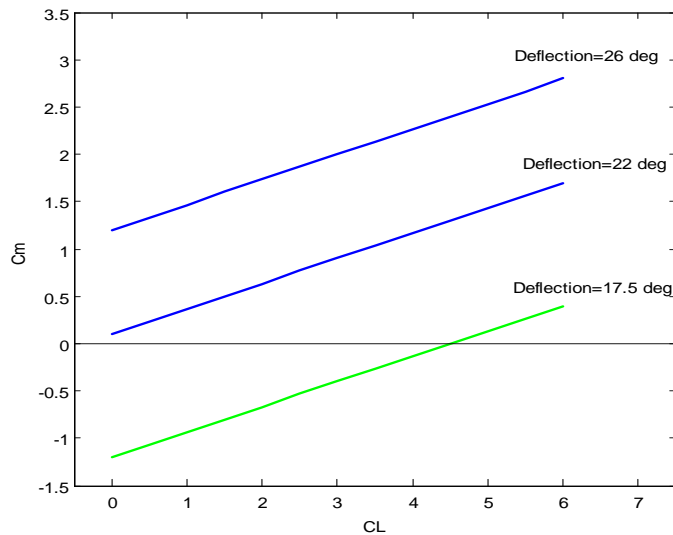


Figure 6.1 - Trim for  $C_{Lmax}$  for Various Elevator Deflections

## 6.2 CENTER OF GRAVITY VARIATION

The aircraft's center of gravity is constantly moving while the aircraft is in flight. This is due to changing angles of attack, fuel consumption and any number of forces an aircraft comes in contact with while airborne. Depicted below in Figures 6.3 and 6.3 are variation of CG location with aircraft weight for the two missions required in the RFP.

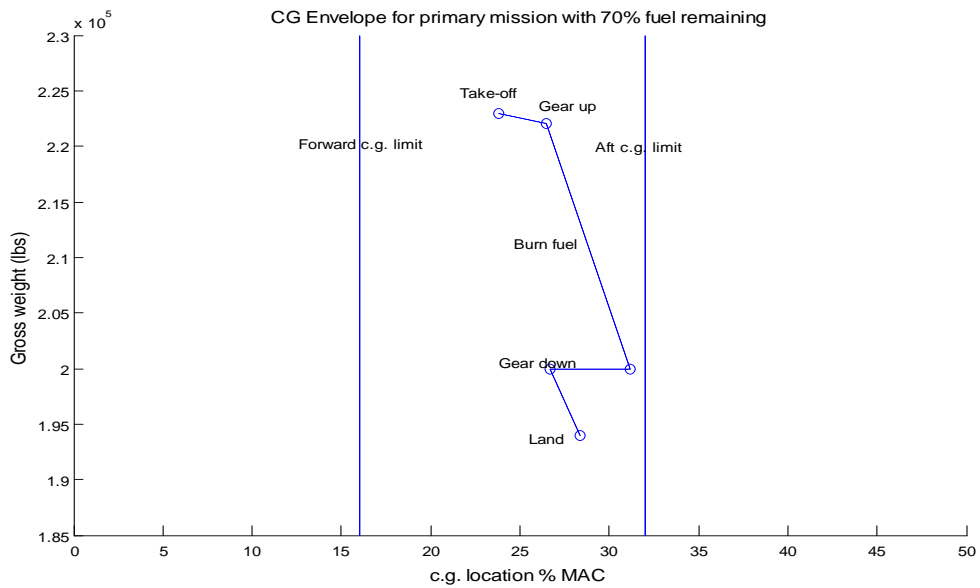


Figure 6.2 - Primary Mission Center of Gravity, Neutral point = 23.8 %MAC

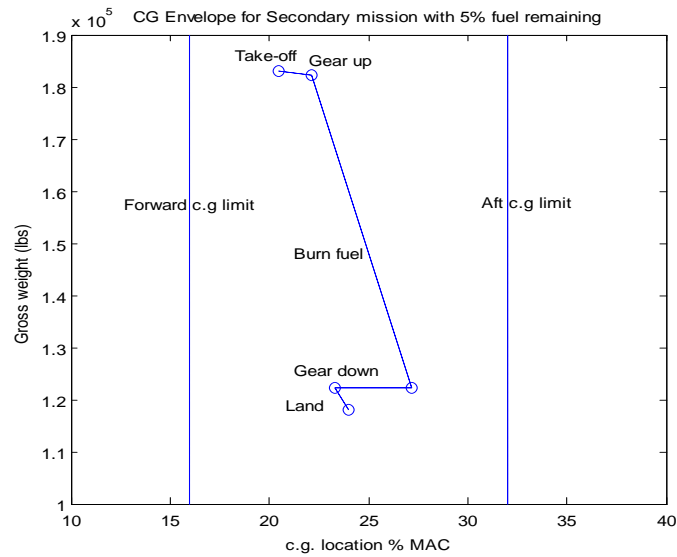


Figure 6.3 - Secondary Mission Center of Gravity Location, Neutral point = 20.5% MAC

## 6.3 DEEP STALL

The Mr. T's namesake comes from its vertical tail, which is a beneficial aspect for ground coverage, but creates another issue with deep stall. Deep stall is a situation where the horizontal tail is directly in the flow of the wing stall, as seen in Figure 6.1. This creates a situation where pitch control becomes inoperable. To prevent this situation, a control situation with an angle of attack limiter is necessary. When the angle of attack reaches values of about  $15^\circ$  the Mr. T is at risk for deep stall. For this reason the control system prevents the pilot from bringing the aircraft to these values of  $\alpha$ .

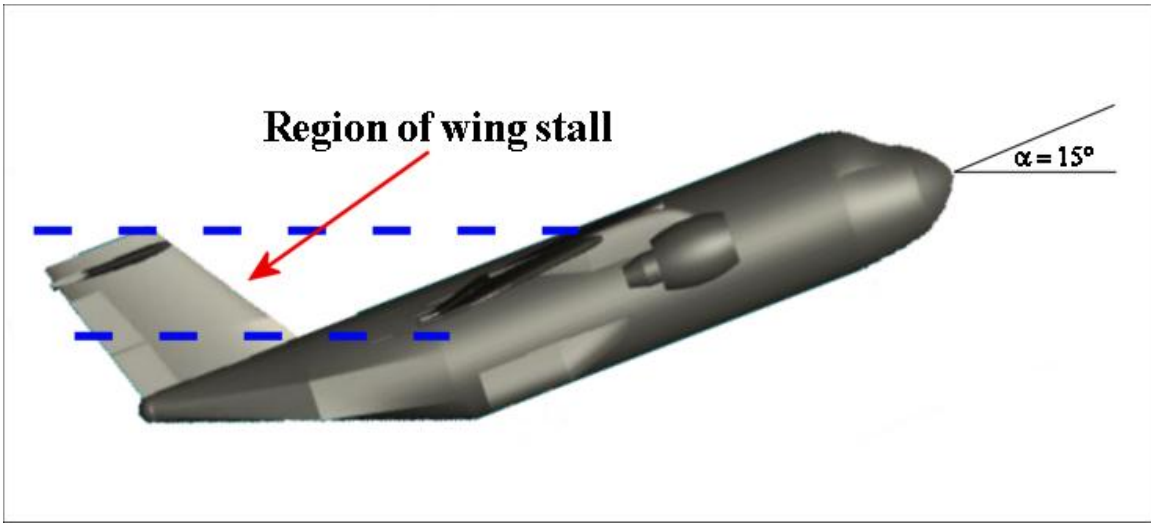


Figure 6.4 – Deep Stall of Mr. T

## 7. PERFORMANCE

### 7.1 REQUIREMENTS

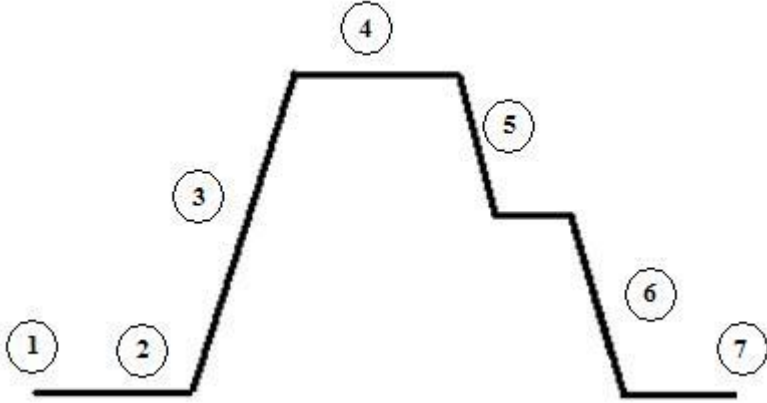
The RFP outlines a number of performance requirements for the aircraft design, but they are all based around a similar goal: short takeoff and landing (STOL) field capability. Consequently, the main drivers for aircraft performance of the Mr. T became balanced field takeoff distance and landing distance. These requirements are covered in the AIAA RFP. The following sections will discuss the performance aspects of the Mr. T aircraft, focusing primarily on takeoff and landing calculations.

### 7.2 OVERVIEW

Most of the calculations performed are based on the first mission of the RFP: the combat mission involving a future deployable armored vehicle (FDAV). This was done for two reasons. First, the combat mission appeared to take a slight precedence over the transoceanic ferry mission, and secondly, the ferry mission does not involve transporting the 25 ton FDAV.

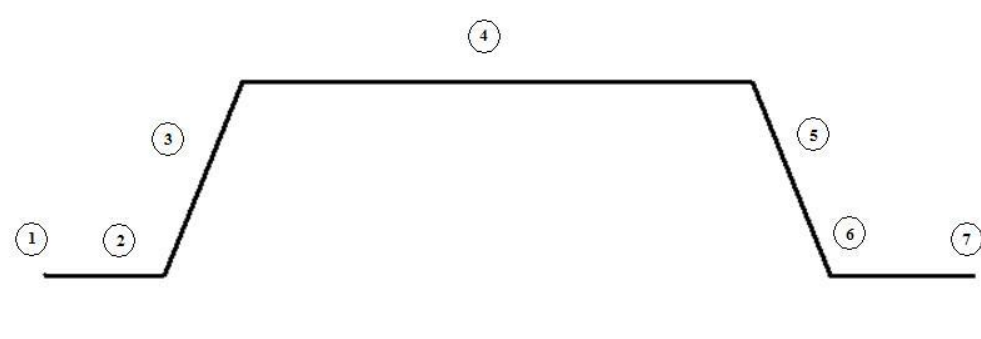
This weight, in addition to an extra 10,000 lbs. accounts for the nominal payload and is slightly larger than a quarter of the TOGW used during calculation. If the Mr. T is able to complete the first mission flawlessly, a considerable drop in weight will allow it to complete the second mission without a problem. Table 7.1 shows the first half of the combat mission, and the second portion simply mirrors this half. Table 7.2 shows the entire ferry mission. Together, these two tables graphically portray each mission broken down into segments and the approximate estimates that coordinate with those segments.

Table 7.1 – Performance estimates for the combat mission



Mission Segment	Mach	Altitude (ft.)	Distance (nmi)
1. Warm-up, taxi, takeoff	0 to 0.4	0	-
2. Accelerate to climb speed	0.4 to 0.74	0	0.29
3. Climb to BCA	0.74 to 0.82	28,000	18.37
4. Cruise at BCA	0.82	30,000	481.63
5. Descend	0.82 to 0.6	1000	100
6. Descend to sea level	0.6 to	0	1.26
7. Landing	-	0	0.34

Table 7.2 – Performance estimates for the ferry mission



Mission Segment	Mach	Altitude (ft.)	Distance (nmi)
1. Warm-up, taxi, takeoff	0 to 0.4	0	-
2. Accelerate to climb speed	0.4 to 0.74	0	0.18
3. Climb to BCA	0.74 to 0.82	28,000	14.75
4. Cruise at BCA	0.82	30,000	3185.25
5. Descend to sea level	0.82 to 0	0	1.26
6. Landing	-	0	0.34
7. Taxi and park	-	0	-

## 7.3 TAKEOFF

The takeoff sequence for the Mr. T can be broken down into two segments: the ground roll portion and the climb portion. Figure 7.1 represents this graphically.

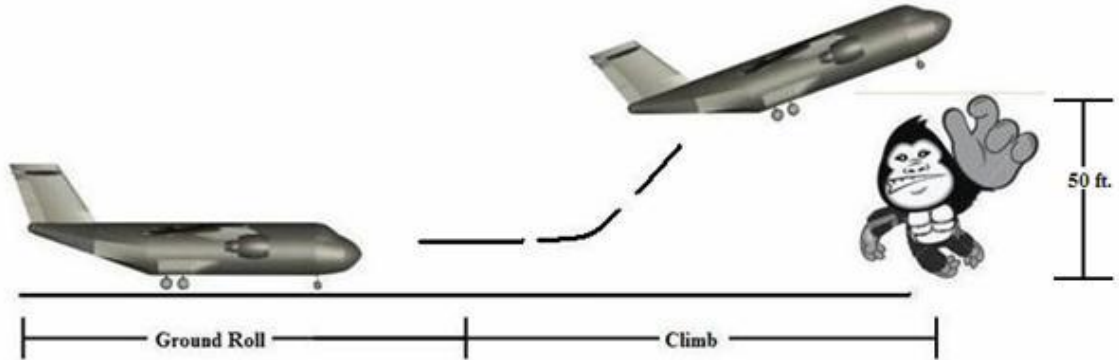


*Figure 7.1 - Breakdown of takeoff segment*

In order to determine whether or not the Mr. T would be able to takeoff within the stipulated balanced field length (BFL) of 2,500 ft., a program was formulated using Matlab to calculate this distance, as well as a number of other factors critical to performance. The BFL is defined as the total takeoff distance, which includes the clearance of the obstacle, an engine becoming inoperable at a specific decision speed, and presuming that the distance to brake is equal to the distance to continue the takeoff. If the engine becomes inoperative prior to the decision speed, the pilot can easily stop the aircraft, but if this occurs after the decision speed has been reached, the pilot must continue the takeoff procedure. The inputs of the program consist of a few constants such as gravity and density, but the majority is key inputs specific to the Mr. T. They include figures such as weight, wing area, maximum lift coefficient, and thrust equation

coefficients. The RFP states that takeoff must be performed under “combat rules” which simply require that the total takeoff distance be equal to the clearance of a 50 ft. obstacle from a standing start. Also, the option of a possible headwind or tailwind was taken into consideration, although the RFP did not specify any type of wind during takeoff.

The following is a Table 7.3 summarizes the crucial outputs from the Matlab program concerning the takeoff performance of the Mr. T:

*Table 7.3 – Normal Takeoff Performance*

<b>Normal Takeoff</b>	
Rotation Velocity	137.58 ft/s
Liftoff Velocity	168.47 ft/s
Velocity over Obstacle	184.72 ft/s
Total Takeoff Distance	1783.54 ft/s
Total Takeoff Time	18.20 ft/s
<b>Balanced Field Length</b>	<b>2172.98 ft</b>

From this table, it is clear that the Mr. T has a BFL of less than the stipulated 2,500 ft. by approximately 327.02 ft. Again, the BFL requirement remains the same for the transoceanic ferry mission, but with the loss of about 60,000 lbs., the balanced field length can only decrease from 2,172.98 ft. The table also outlines a few other characteristics worthy of note including a total takeoff distance of 1783.54 ft. and a total takeoff time of 18.20 seconds. Figure 7.2 graphically shows the progression in distance and velocity, both in the x- and y- directions as time increases from zero.

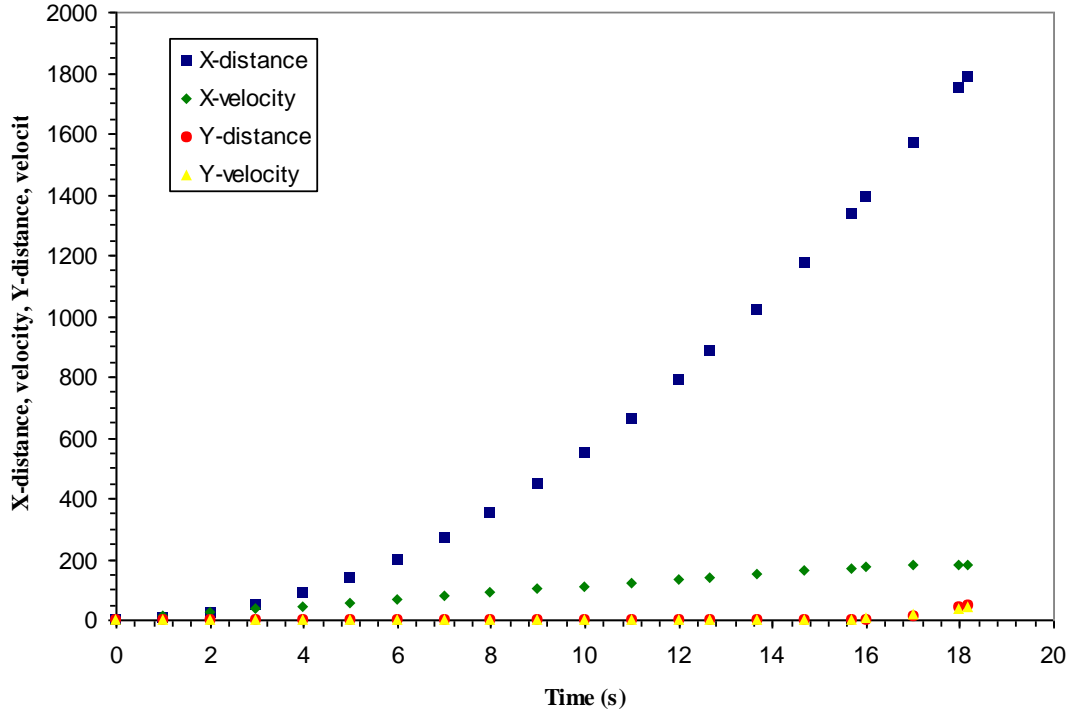


Figure 7.2 - X, Y Distances and Velocities vs. Time

## 7.4 LANDING

The landing sequence for the Mr. T can be broken down into three segments: the approach portion, the touchdown portion, and the braking portion. Figure 7.3 represents this graphically.

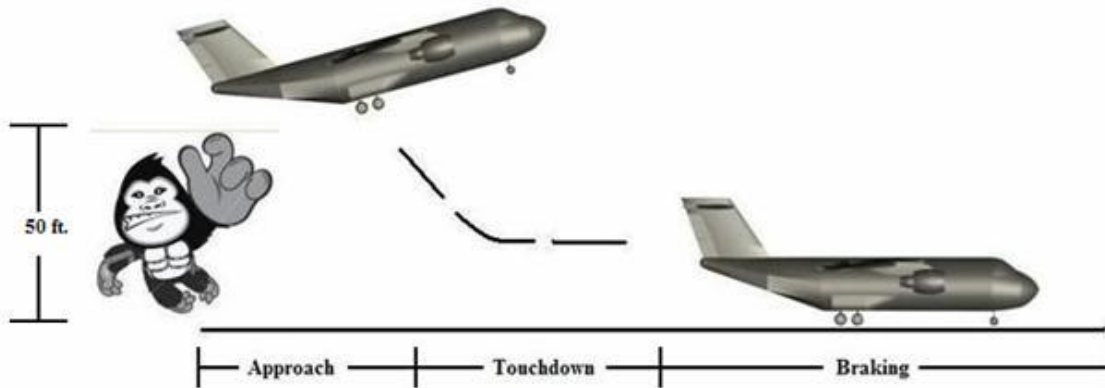


Figure 7.3 - Breakdown of landing segment

When analyzing the landing performance capabilities of the Mr. T, three primary things were taken into consideration: wind, obstacles, and the California Bearing Ratio (CBR). The RFP states that the aircraft must be able to land in a 25 knot crosswind with a 5 knot tailwind component. This is because the landing zone could possibly be oriented in a direction that is not optimal due to combat conditions or other various effects. As far as obstacles are concerned, the RFP states that 50 ft. obstacles are located 250 ft. from either end of the runway similar to what was mentioned in the takeoff section. Both the wind and the 50 ft. obstacles are factored into a Matlab program that was used to determine landing performance. The landing zone consists of a blacktop area of 3000 ft. by 150 ft., and it has a CBR of 4-6. The CBR test is basically a strength test that compares the bearing capacity of a material with a high quality stone material that has a CBR of approximately 100%. A ratio of 4-6 correlates to grained soil, almost similar to the texture of fine dirt or sand. Since this dictates the type of landing gear that can be used, a discussion of the extensive research that was carried out will be discussed in a later section.

The following Table 7.4 summarizes the crucial outputs from the Matlab program concerning the landing performance of the Mr. T:

Table 7.4 – Normal Landing Performance

<b>Normal Landing</b>	
Stall Velocity	123.82 ft/s
Approach Velocity	148.58 ft/s
Touchdown Velocity	136.20 ft/s
Vertical Touchdown Velocity	17.58 ft/s
Horizontal Touchdown Velocity	135.06 ft/s
Approach Angle	7.41°
<b>Total Landing Distance</b>	<b>2096.97 ft</b>

These results demonstrate that the Mr. T will easily land within the stipulated 3000 ft. area of blacktop by approximately 903.03 ft. Other points worthy of note are the different velocities listed in the table. Because the Mr. T must have STOL field capabilities, both the vertical touchdown velocity and the approach angle are higher than normal. Since the Mr. T has to land in a shorter distance, the vertical touchdown velocity needs to be rather high, and this in turn will lead to a steeper approach angle.

## 8. STRUCTURE AND MATERIALS

### 8.1 STRUCTURAL CONFIGURATIONS AND MATERIALS

The main driver for structural configuration is the austere take-off objective of take-off under 2500 feet balanced field length and landing within 3000 feet. Secondary drivers are simplicity of design, low weight, and low cost. Material selection is influenced heavily by the strength needs and lower weights.

### 8.2 LOAD LIMIT

Structural components of the ‘Mr. T’ were designed to withstand loads designated by Mil specs and FAA regulations. The maneuver and gust load limits of the flight envelope are shown in the austere transport Vn diagram below.

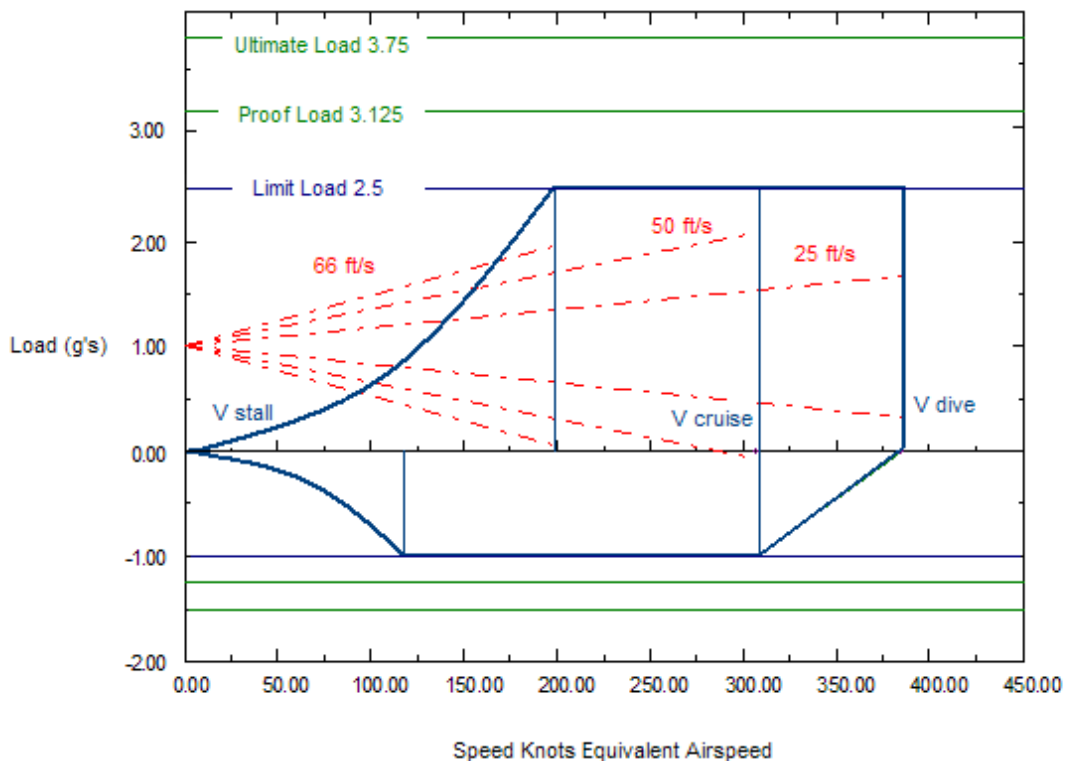


Figure 8.1 - Vn Diagram

Military cargo regulations require a structural load limit of +2.5, -1. The ultimate load beyond the limit loads is the point at which failure is certain after 3 seconds of constant loading (Sharp). FAR 25 regulations establish the gust velocity as 66 ft/s, the design speed as 50 ft/s, and the dive speed as 25 ft/s. The high wingloading of Mr. T places the limit load outside the effects of the gust loads, which therefore do not extend the flight envelope of the austere transport. Operation of the aircraft outside the flight envelope is not protected by the safety factor of 1.5 and operation above the ultimate load is likely to cause structural failure.

### **8.3 MATERIALS**

Initial weight and performance calculations were based on the austere transport being constructed entirely of aluminum, mainly Al 2024-T3 for the aircraft skin, 6061-T6 and 7075-T6 for support structures. The main driver for a change in aircraft materials was weight reduction. The goal for materials was to remain cheap and as until the aircraft performance requires more specialized materials to satisfy the RFP. This proved necessary in initial take-off performance, which proved that the aircraft initially could not take-off in 2500 feet. To shorten the take-off, weight was removed from the wings by constructing the wings from carbon-fiber epoxy composites. In a typical aircraft the graphite epoxy composite replacement for aluminum reduces weight by 25%. The weight reduction in the wings shortened take-off by over 200 feet.

The use of composites and other exotic materials is limited on Mr. T. In 2005, carbon reinforced plastic composite prices rose over 150% due to the high demand in the commercial aviation industry (“In Composite Race”). In addition to prices rising, composite materials tend to cost three to five times more than aluminum. Costs are higher as a result of testing, production, tooling, and quality control (Raman). Composites are subject to cracks and

delamination that are difficult to detect. Joints are more difficult to create in composite parts since they cannot be riveted or welded. Composites are brittle, which causes more structural break-up in a crash or other incursion during operation. Aluminum sustains 24 times the deformation and 65 times the energy absorption capacity than composites. Humidity also decreases the strength of the composite epoxy.

Composites are superior to aluminum in stiffness, fatigue resistance, and corrosion resistance and are therefore used in areas of Mr. T susceptible to failure due to cyclical loads. These materials have 25-35% lower weight than aluminum and require fewer parts. Aluminum-lithium alloys are an alternative to composites since they are 10% lighter and 10% stiffer than regular aluminum with superior fatigue performance. Aluminum-lithium has been used since the 1950's in military aircraft. The cost of aluminum lithium is at least three times as high as other aluminum alloys and cannot be recycled. Therefore, we chose to not use it on Mr. T, instead the structure is composed of composites and conventional aluminum alloys.

Titanium alloy Ti-6Al-4V is used in landing gear because of its superior strength to both aluminum and graphite/epoxy composites. Titanium is highly resistant to corrosion which affects the integrity of the gear's ability to handle loads associated with landing. Titanium is also used for fasteners in composites since it won't cause corrosion with the graphite. Aramid/Epoxy composites are resistant to heat and impact damage, making them useful in engine structural applications. The radome of the austere transport requires a material with no electrical conductance making a quartz/epoxy the appropriate material.

Table 8.1 – Characteristics of Materials

Material	E (psi) x10 <sup>6</sup>	Density (lb/in <sup>3</sup> )	Ultimate Tensile Strength (psi)	Fatigue Strength (psi)	Shear Strength (psi)
Al 2024-T3	10.6	0.101	50,000	20,000	41,000
Al 7150-T6	10.4	0.102	83,000	25,000	48,000
Al 7178-T6	10.4	0.102	88,000	21,800	52,200
Ti-6Al-4V	16.5	0.16	138,000	34,800	79,800
Fiber Metal Laminate	13.0	0.093	168,200	--	--
Graphite/ Epoxy	20.3	0.058	210,000	--	--
Aramid/ Epoxy	12.6	0.052	203,000	--	--

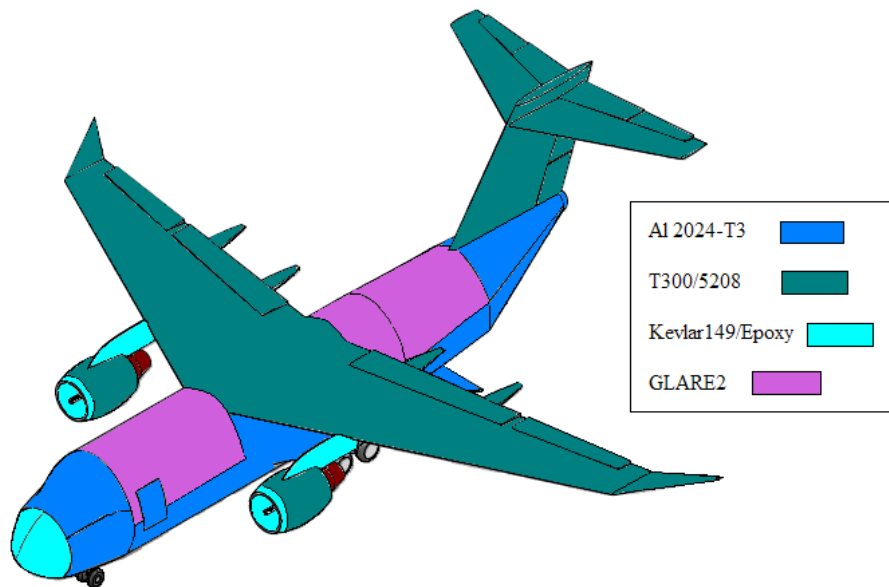
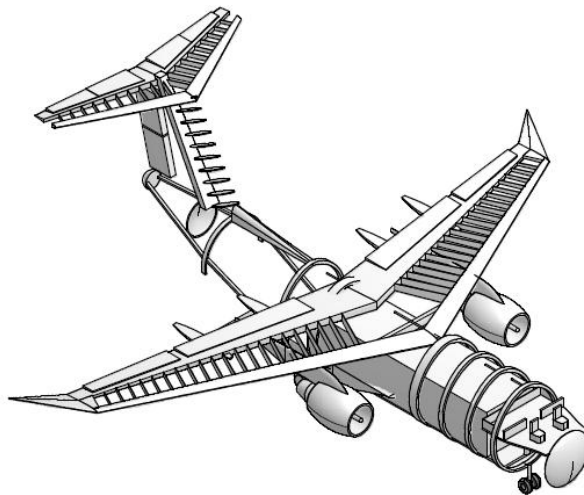


Figure 8.2 – Materials Placement

## 8.4 INTERNAL STRUCTURE

The austere transport must have a structure that will not fail until the ultimate load has been surpassed on the flight envelope, while minimizing cost associated with the complexity and number of parts. This minimizes weight, a crucial element in austere take-off performance. Loads must be distributed from the wings, tail, and landing gear through the aircraft body and it is done through the use of seven bulkheads. Another two specialized bulkheads support the pressurization of the fuselage. The flight envelope allows a maximum bending moment of 8.6 million ft-lb per wing that is supported by two integrally machined spars and graphite/epoxy composite skin.



*Figure 8.3 - Internal Structure*

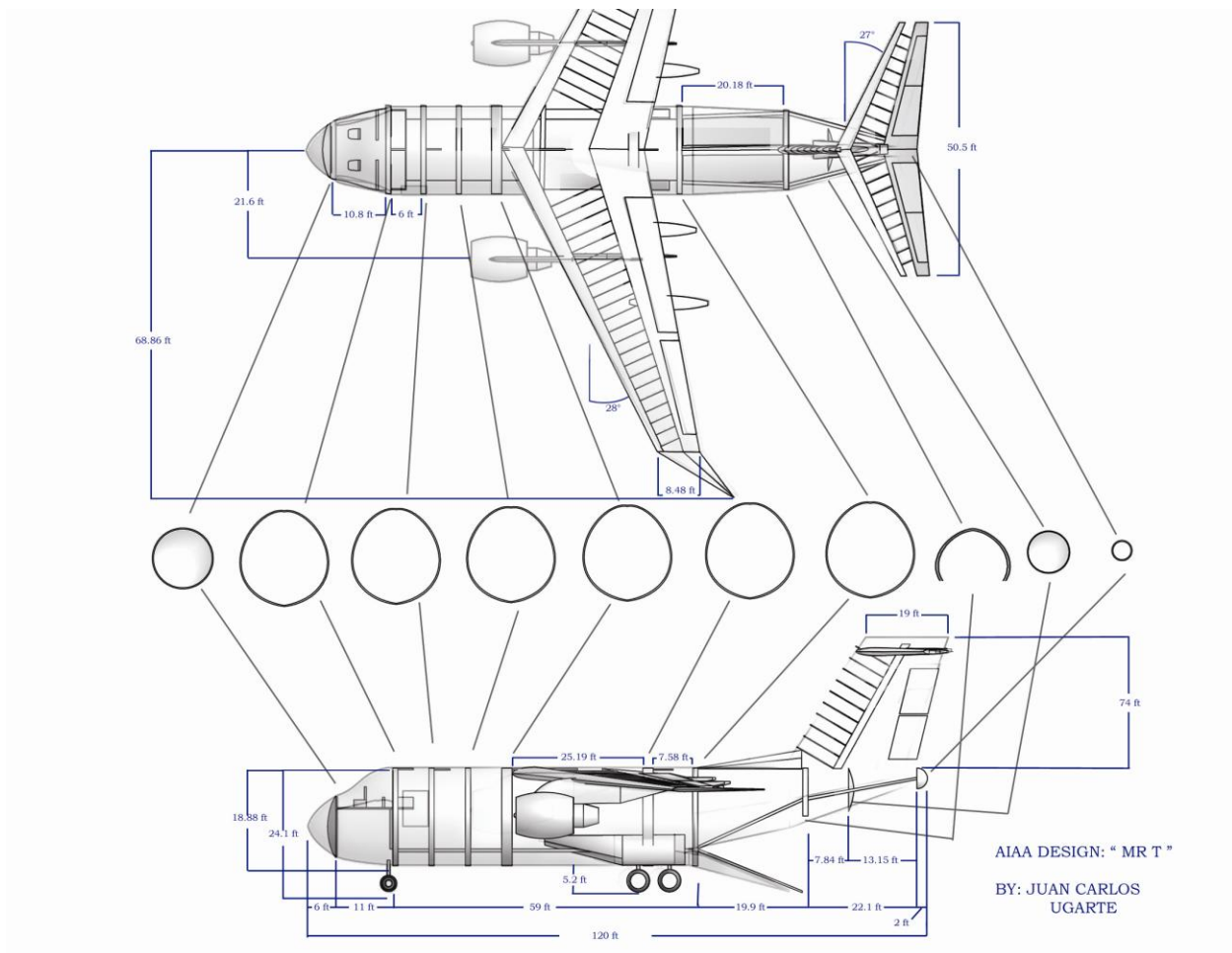


Figure 8.4 - Bulkheads

## 8.4.1 FUSELAGE

The 120 ft long monocoque fuselage is held in flight by two reinforced bulkheads made from high strength Al 7150-T6 attached to the overhead wing. The foremost and rearmost bulkheads support stresses caused by cabin pressurization stresses. The five remaining bulkheads distribute stresses to the fuselage skin caused by the landing gear, cargo floor, cargo door, cargo itself, and other stresses caused by weights and cutouts. The skin of the aircraft is 0.05 inch thick, stiffened, fatigue resistant, Al 2024-T3 to carry shear, transverse, and torsional loads experienced by the aircraft during operation. The skin is integrally stiffened with stringers every

8 inches. This skin covers 5 inch thick Al 7150-T6 rings spaced 20 inches apart as suggested by (Neu). Longerons are compression resistant Al 7178-T6 to counteract bending stresses in the fuselage. Upper fuselage areas especially susceptible to fatigue due to cyclical tensile loads from bending and cabin pressurization will be composed of highly fatigue resistant GLARE 2 fiber metal laminate.

### **8.4.2 WINGS**

The highest bending moment the wing receives in the flight envelope with a factor of 1.5 is 8.6 million ft-lb. Wing surface graphite epoxy composite T300/5208 skin carries the bending moment to two spars, placed at the 15% and 60% chord location. The upper and lower surfaces of the wing are made from the graphite composite. These two spars are made from high compressive strength Al 7178-T6. The wings are given an anhedral angle of 5 degrees for extra stress support in flight. Spars are integrally machined webs to inhibit internal crack propagation with a maximum web thickness of  $t/c = 0.12$ . The ribs are made from Al 7150-T6 with a minimum web thickness of 0.04 to resist fuel sloshing. Ribs are placed in the wing every 30 inches. All ribs found in the aircraft are placed parallel to the leading edge to reduce rib length and weight. The volume in the wing between spars is 2525 ft<sup>3</sup> for fuel tanks. Flaps and ailerons are graphite composite because of its high stiffness.

### **8.4.3 EMPENNAGE**

The T-tail design incorporated into Mr. T requires 1.5 times the torsional stiffness at the root and 40 times the torsional stiffness than a conventional tail. The skin of the horizontal stabilizer and vertical tail will be made from graphite epoxy composite to meet stiffness requirements and to handle torsion, as well as reduce the increased weight of a T-tail over a

conventional tail. The elevators and rudder are also graphite composite because of its high stiffness. The vertical tail is supported by two Al 7150-T6 spars located at the 10% and 60% chord length with Al 7150-T6 ribs located every 26 inches. The horizontal tail has spars at 10% and 65% chord with ribs every 30 inches.

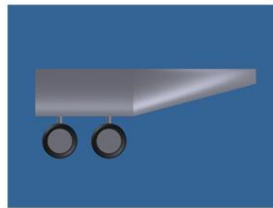
#### **8.4.4 NACELLES**

The engine nacelles are primarily made from graphite epoxy composite with a cowling composed of the aramid fiber epoxy composite. The ultra high strength aramid fiber, Kevlar 149, is used in the composite because of its extreme impact damage resistance and heat resistance. The pylon supporting the engine and nacelle is Kevlar149 epoxy composite to resist dynamic fatigue experienced during flight and engine operation.

#### **8.4.5 LANDING GEAR**

The landing gear size is based on a number of variables, the main one being weight. The weight of the aircraft is the starting point, this TOGW must be multiplied by 7% to comply with FAR 25 regulations, and then a general rule of thumb is to also increase the weight by 25% for possible future modifications to the aircraft. This brings the weight of the aircraft from 223,200 lbs to 294,624 lbs. According to Raymer, aircraft weighing between 200,000 and 400,000 lbs will generally employ a four-wheeled bogey. With this in mind we calculated the size of the tires assuming that there are two wheels on a single strut on the nose gear and eight wheels on two four wheeled bogeys on the rear landing gear. Assuming the general rule that 10% of the weight of the aircraft will be supported by the nose gear and that 90% of the weight will be supported by the rear gear, we calculated that the nose gear needs to be able to support 14,731.2 lbs per tire and the rear gear needs to support 33,145.2 lbs per tire. Using chart 11.2 in Raymer

and Three-Part Name tires, we found the tire size necessary to support this weight. Once this was calculated, we multiplied the diameter and the width by 30%, to ensure the ability to land on a CBR of 4-6 landing surface as specified by the RPF. Once all the calculations were made and the tire size was increased, we found that the nose gear will require a 37x14.0-14 tire and the rear gear will require a 52x20.5-23 tire (where the first the sizes are as follows: diameter x width – wheel size) as seen in Figure 8.5.



## Landing Gear



The picture above shows the main landing gear pods which are attached to the aircraft at the main landing gear position.

The main landing gear will fold in after take off and vise versa for landing in the form above. The nose landing gear will simply fold backward after take off and vise versa for landing.

*Figure 8.5 – Landing Gear*

## 9. SYSTEMS

### 9.1 FLIGHT CONTROL SYSTEMS

Our aircraft will make use of the fly-by-light (FBL) technology for our flight control system. FBL has many advantages over the more conventional fly by wire system. It employs fiber optic technology to send and receive information to the actuators at the control surfaces. The fiber optics allows for more data transfer and thus more sophisticated signals to the actuators. This increased data flow can more effectively limit pilot error and increase stability and flight performance. Along with increased flight performance, FBL is especially practical for military aircraft because of its immunity to electromagnetic interference (EMI). A conventional fly by wire system employs electrical circuits which are prone to electromagnetic pulses, a weapon that could very conceivably be used by the enemy. Properly functioning flight control systems are crucial in STOL scenarios where the risk of EMI is greatest, therefore making the FBL immunity extremely practical and effective. In addition to these benefits, FBL can reportedly reduce the weight of flight control systems by around 25% as well as significant volume and cost reductions (Dawson). In a transport aircraft any weight reduction means less fuel and longer range, which can be crucial constraints on a mission.

### 9.2 AVIONICS

We will use the Rockwell Collins Flight2 FMS 800 integrated avionics system. The decision for this was based on the need for a reliable system that performs the necessary flight computational data and its applicability to C-5 and C-130 aircraft, which are both similar in design and function to ours. The FMS 800 is a flight operations system with navigation and

guidance functions, flight management systems, and GPS/INS. It also has a multiple product interface, plug and play capability. The pilot interface will include a stick control design because it is smaller and interferes less with the pilot's legs and view of the instrument panels. Our flight deck will also include Heads up display (HUD) for the pilot and co pilot. This will allow for the pilots to have eyes out of the cockpit on landing, which greatly reduces potential for error. The avionics will also include an alpha limiter to prevent pilot error and stall with the angle of attack.

### 9.3 NAVIGATION

A Honeywell Multi-Function Radar Display (MFRD) and Enhanced Ground Proximity Warning System (EGPWS) were chosen as navigation systems. The MFRD includes weather and traffic radar, as well as terrain and navigation mapping. These systems were chosen because of their ability to integrate aircraft safety information in all environments in a clear and integrated format and for their high reliability (Multi-Function).

### 9.4 COMMUNICATIONS

For the communication system, we chose the AN/ARC-232(V) STARBLAZER from Raytheon. It is qualified to military standards and employs VHF and UHF single-band air traffic controls and radio systems. The system also supports airborne, multi-band, multi-mission, and voice and data network-capable communications systems in a single package (AN ARC-232).

### 9.5 FUEL TANKS

The maximum amount of fuel needed by Mr. T to perform the missions required by the RFP is 65,000 lbs. This converts to a maximum fuel volume of almost 1300 ft<sup>3</sup> of fuel for the PW4050 engines, or 650 ft<sup>3</sup> of fuel per wing. The upper wing design allows for the fuel tanks to

extend through the fuselage and take advantage of a fuel tank of maximum thickness (Figure 9.1). The fuel tank is an integral design rather than a bladder tank to reduce weight. Survivability was an important factor in fuel tank design in the austere transport since the aircraft may be fired upon. Current self-sealing designs rely on a rubberized bottom third section of the tank with an inerting system to avoid a fuel explosion. This method may take up to 2 minutes to fully seal which may lead to ignition of leaking fuel (Ball). A more promising method is the addition of Surlyn ionomer sheet to the bottom of fuel tanks (Glodsmith). The heat from an impact with this sheet would seal the fuel tank instantly, making sure no leaking fuel can ignite. This method is not used on Mr. T, however, because the ionomer still reacts with fuel. Future upgrades may make the ionomer self-sealing tanks the better option for Mr. T.

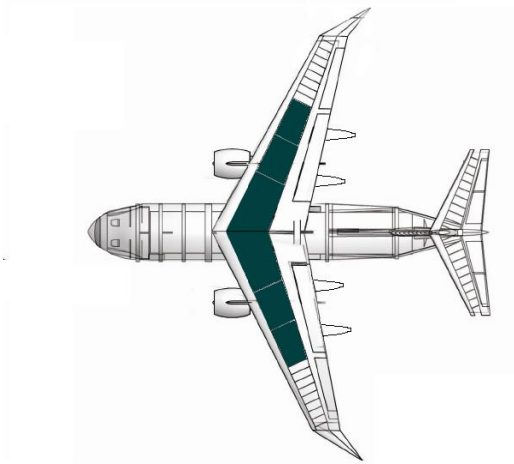


*Figure 9.1 – Fuel Tanks*

## 9.6 REFUELING

A probe and drogue refueling system will be implemented on our aircraft. The probe and drogue system uses an extendable probe that meets a drogue and line being towed behind a refueling aircraft. This will allow for increased range on missions because they will not be

limited to just the fuel at takeoff. The aircraft will also contain a fuel dumping system to meet landing weight requirements.

## 9.7 ENVIRONMENT AND ELECTRIC SYSTEMS

An Environmental Control System and a Power System are used to convert fuel energy into power to control cabin atmosphere, deliver pneumatic power to the pylon for engine starting, and provide auxiliary electrical power. For primary electrical power, turbine generators are run from each engine. These provide AC power which is converted to DC for use by the aircraft's systems. The auxiliary power unit (APU) is designed for air transport aircraft and is used to provide backup power in case there is main power system failure. It also provides full electrical power for the aircraft in emergencies. Controlling cabin environment requires an air conditioning system and a cabin pressure control system, while the pneumatic system moves compressed bleed air throughout the aircraft. A Hamilton Sundstrand Aerospace Integrated Air Management and Power System was chosen to simplify system interfaces, reduce the weight, cost, and number of parts, and optimize overall system performance. Hamilton Sundstrand is a major supplier of air management systems for military fighters and transports and their systems are found on the Boeing 777 and F-16 (Air Management).

## 9.8 AIR DEFENSE SYSTEMS AND SAFETY

Specific safety issues come into play when the aircraft is involved in a military mission. The Northrop Grumman QRC84-02A infrared countermeasures system will be used to jam incoming missiles that use infrared detection. The AN/ALE 47 automatic flare dispenser will also be used provide decoy heat for heat seeking missiles and hopefully save the aircraft. An NC1151 On-Board Inert Gas Generation System (OBIGGS) by Carleton Life Support Systems

prevents ignition of fuel tank vapors by providing a nitrogen enriched air blanket around the engines to displace flammable fuel/air mixtures (NC1151). The Identification Friend or Foe (IFF) system will allow pilots to distinguish between hostile targets and friendly unknown forces. There will be a life raft ejection system in case of emergencies or crashes into water (Manneville)(Identification).

## 9.9 NOISE MITIGATION

There are several reasons why our aircraft will need to have a form of noise mitigation. It may conceivably be flying over or landing near an enemy occupied zone, if the aircraft is quieter it will have a smaller chance of being detected and damaged or shot down by enemy anti aircraft weaponry.

The major sources of noise occur during takeoff and landing and stem from the fan noise emitted by the engine and the turbulent airflow coming off the high drag surfaces used to slow the plane. We are implementing a relatively more quiet high lift turbo fan to reduce an extent of the noise. For noise produced by high drag surfaces on the airframe there is not much that can be done because the drag is necessary to slow the plane down on approach (Manneville). The landing gear also produces a lot of noise when it is deployed because it is not aerodynamic at all. There is research being done on toboggan shaped fairings that could be placed in front of the landing gear to decrease noise. According to NASA research a design produced by Goodrich could reduce as much as 4 decibels of noise from the main landing gear. This technology is still undergoing research though and may not yet be ready for implementation(Braukus).

## 9.10 LAVATORY

Because of the nature of transport missions, flights potentially can be very long. For crew comfort, it is worth implementing a lavatory system. We will use a standard 36 x 36 inch lavatory. It will use vacuum flush and will be a self contained system. It must be serviced after every flight.

## 10. COSTS

The RFP states that flyaway and direct operation cost requirements are to be estimated for the production of 150, 500 and 1500 aircraft units. The methods used to estimate costs are outlined in *Aircraft Design: A Conceptual Approach* by Raymer. The RFP requires Research, Development, Test and Evaluation Costs but also flyaway costs. This is to be estimated with production quantities of 150, 500, and 1500. For the estimates we assumed four test flight aircraft. All cost estimates are based on the 2007 dollar value.

The following estimates are based on the follow constants: empty weight, maximum velocity, number to be produced in five years, number of test aircraft, total number of engines, engine maximum thrust, engine maximum Mach number, turbine inlet temperature, and avionics cost.

*Table 10.1 - Constants for Costs Analysis*

<b>Parameter</b>	<b>Value</b>
Empty Weight	101111 lbs.
Maximum Velocity	471 knots
# to be Produced	150, 500, 1500
# of Flight Test Aircraft	4
Total Number of Engines	300, 1000, 3000
Engine Maximum Thrust	52000 lbs.
Engine Maximum Mach	0.8
Turbine Inlet Temp	2500 deg R
Avionics Cost	\$6000 x weight of aircraft

RDT&E costs are based off the number of hours it traditionally takes to develop an aircraft with these parameters and then multiplying those numbers of hours by the hourly rate for those corresponding labor costs. The flyaway costs, also known as the acquisition cost, are the capital required to purchase an entire production of aircraft.

*Table 10.2 - RDT&E Cost Analysis for 150, 500, and 1500 aircraft*

<b>RDT&amp;E Category</b>	<b>Cost for 150 (\$)</b>	<b>Cost for 500 (\$)</b>	<b>Cost for 1500 (\$)</b>
<b>Engineering</b>	2,217,755,196	2,698,626,874	3,227,851,939
<b>Tooling</b>	1,364,706,832	1,873,080,643	2,500,572,011
<b>Manufacturing</b>	4,121,056,932	8,916,078,634	18,030,535,044
<b>Quality Control</b>	347,523,650	751,881,919	1,520,492,791
<b>Total</b>	8,051,042,611	14,239,668,070	25,279,451,784

*Table 10.3 - Flyaway Cost Analysis for 150, 500, and 1500 aircraft*

<b>Flyaway Category</b>	<b>Cost for 150 (\$)</b>	<b>Cost for 500 (\$)</b>	<b>Cost for 1500 (\$)</b>
<b>Development Support</b>	346,067,701	346,067,701	346,067,701
<b>Flight Test</b>	79,602,077	79,602,077	79,602,077
<b>Manufacturing Materials</b>	2,013,025,012	5,267,800,130	12,672,116,916
<b>Engine Production</b>	2,189,321,587	7,297,738,624	21,893,215,871
<b>Avionics</b>	749,232,510	749,232,510	74,923,510
<b>Total</b>	5,377,248,888	13,740,441,041	35,740,235,074

*Table 10.4 - RDT&E + Flyaway Costs for 150, 500, and 1500 aircraft*

<b>Number to be Produced</b>	<b>Total Cost (\$)</b>
150	13,428,291,499
500	27,980,109,112
1500	61,019,686,859

# 11. CONCLUSION

The A-team presents Mr. T as its proposal for an Inter-Theatre Tactical Transport with Austere STOL Capability, which fulfills all RFP requirements for the 2006/2007 AIAA undergraduate design competition. Mr. T is a relatively low cost solution for a STOL transport featuring a high mounted wings and T-tail configuration with externally blown flaps. Modern low density high stiffness materials are found in fuselage, wings, empennage, and landing gear as needed in addition to conventional aluminum alloys to provide for a low weight cost efficient air transport

Mr. T is capable of operating in areas of commercial airspace on the most modern runways within the continental United States as well as extreme runways as short as 2500 ft in the more remote parts of the planet. In flight refueling systems allow Mr. T to reach any airfield on the planet. The United States armed forces will be able to use the versatility of Mr. T to transport the Future Deployable Vehicle or cargo to anywhere in the world or perhaps use the tactical transport for other unforeseen missions.

*Table 11.1 – Compliance to Design Drivers*

<b>Criterion</b>	<b>RFP Requirement</b>	<b>Mr. T Capability</b>	<b>Compliance</b>
<b>Primary Mission</b>			
Warm-up and taxi at idle power	8 minutes	8 minutes	Yes
Take-off fuel allowance	2 minutes of operation at max takeoff power	2 minutes of operation at max takeoff power	Yes
Balanced Field Length Takeoff	2500 ft	2173 ft	Yes

Cruise/climb to best cruise altitude		4270 ft/min climb 30,000 ft altitude	Yes
Cruise Mach #	>0.8 for 500 nautical miles	0.82 for 500 nautical miles	Yes
Descent	1000 ft for 100 nautical miles at Mach 0.6	1000 ft for 100 nautical miles at Mach 0.6	Yes
Clear obstacle at a distance of 250 ft from runway end at take-off	Height of 50 ft	Height of 210 ft	Yes
Clear obstacle at a distance of 250 ft from start of runway during landing	Height of 50 ft	Height of 84 ft	Yes
Crosswind landing	25 knots	25 knots	Yes
Tailwind landing	5 knots	5 knots	Yes
Balanced Field Length Landing	2500 ft	2097 ft	Yes
<b>Transoceanic Ferry Mission</b>			
Warm-up and taxi at idle power	8 minutes	8 minutes	Yes
Take-off fuel allowance	2 minutes of operation at max takeoff power	2 minutes of operation at max takeoff power	Yes
Balanced Field Length Takeoff	2500 ft	2173 ft	Yes
Cruise/climb to best cruise altitude		4270 ft/min climb 30,000 ft altitude	Yes
Cruise Mach #	>0.8 for 32500 nautical miles	0.82 for 3200 nautical miles	Yes
Balanced Field Length Landing	2000 ft	1368 ft	Yes
Taxi and idle	10 minutes	10 minutes	Yes

Missed approach or Diversion	150 nautical miles	150 nautical miles	Yes
Diversion hold	45 minutes at 5000 ft	45 minutes at 5000 ft	Yes

## WORKS CITED

Air Management Power Systems. 2005. 6 April 2007 <[http://www.hamiltonsundstrandcorp.com/hsc/details/CLI1\\_DIV22\\_ETI3026,00.html](http://www.hamiltonsundstrandcorp.com/hsc/details/CLI1_DIV22_ETI3026,00.html)>.

American Institute of Aeronautics and Astronautics. 2007. 12 April 2007 <[www.aiaa.org](http://www.aiaa.org)>.

AN ARC-232(V) Starblazer Airborne VHF UHF Multi-band Communications System. 2007. 6 April 2007 <[http://www.raytheon.com/products/starblazer\\_airborne/](http://www.raytheon.com/products/starblazer_airborne/)>.

AN/QRC-84. 2007. 6 April 2007 <<http://www.globalsecurity.org/military/systems/aircraft/systems/an-qrc-84.htm>>.

Ball, Robert E. A History of the Survivability Design of Military Aircraft. A434153. Monterey, CA: Naval Postgraduate School, 1998.

Braukus, M. National Aeronautics and Space Administration. 13 April 2005. 5 April 2007 <[http://www.nasa.gov/home/hqnews/2005/nov/HQ\\_05413\\_technologies.html](http://www.nasa.gov/home/hqnews/2005/nov/HQ_05413_technologies.html)>.

California Bearing Ratio. 2000. 27 April 2007 <[http://training.ce.washington.edu/WSDOT/Modules/04\\_design\\_parameters/04-2\\_body.htm](http://training.ce.washington.edu/WSDOT/Modules/04_design_parameters/04-2_body.htm)>.

Cambell, John P., Danny R. Hoad, and William G. Johnson. Powered Lift Aerodynamics and Acoustics. NASA SP-406, 1976.

Campbell, John P. and Homer Morgan. STOL Technology. NASA SP-320, 1972.

Corporation, DAR. "Advanced Aircraft Analysis Software v3.1." 2006.

Dawson, David, et al. Fly-by-Light: The Future of Flight Control Technology. 2005. 6 April 2007 <<http://www.afrlhorizons.com/Briefs/Apr05/VA0412.html>>.

"Federal Aviation Administration." 2003. Regulatory and Guidance Library. 12 April 2007 <[http://rgl.faa.gov/Regulatory\\_and\\_Guidance\\_Library/rgMakeModel.nsf/0/4e1d135907e0ce8686256df1005b1233/\\$FILE/E17NE.pdf](http://rgl.faa.gov/Regulatory_and_Guidance_Library/rgMakeModel.nsf/0/4e1d135907e0ce8686256df1005b1233/$FILE/E17NE.pdf)>.

Glodsmith, Anastasia. "Ionomer Self-Healing Material Applications". 6554. San Diego, CA: AIAA, 2003.

Identification Friend or Foe (IFF) Systems. 2007. 6 April 2007 <[http://www.baesystems.com/ProductsServices/eis\\_nes\\_iff.html](http://www.baesystems.com/ProductsServices/eis_nes_iff.html)>.

"In Composite Race, Jets May Beat Out Bikes." The Wall Street Journal. 24 January 2006.

Manneville, A. "American Institute of Aeronautics and Astronautics." 10 May 2004. Electronic Library. 5 April 2007 <<http://www.aiaa.org/content.cfm?pageid=406&gTable=Paper&gID=18503>>.

Mason, William, comp. Aircraft Systems and Operational Environment: Things We Need to Know About. 6 April 2007 <[http://www.aoe.vt.edu/~mason/Mason\\_f/SD1ACSystems.html](http://www.aoe.vt.edu/~mason/Mason_f/SD1ACSystems.html)>.

Mattingly, Jack D. Aircraft Engine Design. 2nd Edition. AIAA, 2002.

Mattingly, Jack D. et al. Aircraft Engine Design. 2nd Edition. Reston, VA: AIAA Education Series, 2002.

Matweb Material Property Data. 2007. 4 March 2007 <[www.matweb.com](http://www.matweb.com)>.

Multi-Function Radar Display (MFRD). 2007. 6 April 2007 <[http://www.honeywell.com/sites/aero/Displays\\_Electronics3\\_C7282E812-3A8E-422C-A286-2B5804F3A7A9\\_HB889B69E-2CE9-12C4-93F8-053B040D2379.htm](http://www.honeywell.com/sites/aero/Displays_Electronics3_C7282E812-3A8E-422C-A286-2B5804F3A7A9_HB889B69E-2CE9-12C4-93F8-053B040D2379.htm)>.

NC1151 On-Board Inert Gas Generating System (OBIGGS). 2004. 6 April 2007 <<http://www.carletonls.com/productsbu/nc1151.htm>>.

Niu, Michael C.Y. Airframe Structural Design. Burbank, CA: Commilit Press Ltd., 1998.

Pratt & Whitney. 2007. 2007 April 2007 <<http://www.pw.utc.com/>>.

Raman, Raj. The Effects of Advanced Materials on Airframe Operating and Support Costs. Santa Monica, CA: RAND, 2003.

Raymer, Daniel P. Aircraft Design: A Conceptual Approach. 4th Edition. New York, NY: AIAA Education Series, 2006.

Sharp, Maurice L. Behavior and Design of Aluminum Structures. New York, NY: McGraw-Hill, 1993.

"Source Book 2006." Aviation Week Space and Technology 164.3 (2006).